Alternative splicing substantially diversifies the transcriptome during early photomorphogenesis and correlates with the energy availability in arabidopsis

Hartmann, L. and Drewe-Boss, P. and Wiessner, T. and Wagner, G. and Geue, S. and Lee, H.C. and Obermueller, D.M. and Kahles, A. and Behr, J. and Sinz, F.H. and Raetsch, G. and Wachter, A.

Plant Cell
2016 November ; 28(11): 2715-2734
2016 November 01 (first published online: final publication)
doi: 10.1105/tpc.16.00508

Publisher: American Society of Plant Biologists (U.S.A.)

Plant Cell Advance Publication. Published on November 1, 2016, doi:10.1105/tpc.16.00508

LARGE-SCALE BIOLOGY ARTICLE

Alternative Splicing Substantially Diversifies the Transcriptome during Early Photomorphogenesis and Correlates with the Energy Availability in Arabidopsis

Lisa Hartmann,[1] Philipp Drewe-Boß,[2,3] Theresa Wießner,[1] Gabriele Wagner,[1] Sascha Geue,[1] Hsin-Chieh Lee,[1] Dominik M. Obermüller,[1] André Kahles,[2] Jonas Behr,[2] Fabian H. Sinz,[4,a] Gunnar Rätsch,[2,5] and Andreas Wachter[1,#]

[1] Center for Plant Molecular Biology (ZMBP), University of Tübingen, Auf der Morgenstelle 32, 72076 Tübingen, Germany

[2] Computational Biology Center, Memorial Sloan Kettering Cancer Center, 1275 York Avenue, New York, NY 10065, USA

[3] Berlin Institute for Medical Systems Biology, Max Delbrück Center for Molecular Medicine, Robert-Rössle-Strasse 10, 13092 Berlin, Germany

[4] Institute for Neurobiology, University of Tübingen, Auf der Morgenstelle 28, 72076 Tübingen, Germany

[5] Department of Computer Science, ETH Zürich, Universitätsstrasse 6, 8006 Zürich, Switzerland

[a] present address: Baylor College of Medicine, Department of Neuroscience, One Baylor Plaza, Houston, TX 77030, USA

[#] Corresponding author: awachter@zmbp.uni-tuebingen.de

Short title: Light and Sugar Control Alternative Splicing

One-sentence summary: Alternative splicing is an integration point of light and sugar signaling pathways in Arabidopsis.

The author responsible for distribution of materials integral to the findings presented in this article in accordance with the policy described in the Instructions for Authors (www.plantcell.org) is: Andreas Wachter (awachter@zmbp.uni-tuebingen.de).

Abstract

Plants use light as source of energy and information to detect diurnal rhythms and seasonal changes. Sensing changing light conditions is critical to adjust plant metabolism and to initiate developmental transitions. Here we analyzed transcriptome-wide alterations in gene expression and alternative splicing (AS) of etiolated seedlings undergoing photomorphogenesis upon exposure to blue, red, or white light. Our analysis revealed massive transcriptome reprograming as reflected by differential expression of ~20% of all genes and changes in several hundred AS events. For more than 60% of all regulated AS events, light promoted the production of a presumably protein-coding variant at the expense of an mRNA with nonsense-mediated decay-triggering features. Accordingly, AS of the putative splicing factor *REDUCED RED-LIGHT RESPONSES IN CRY1CRY2 BACKGROUND 1* (*RRC1)*, previously identified as a red light signaling component, was shifted to the functional variant under light. Downstream analyses of candidate AS events pointed at a role of photoreceptor signaling only in monochromatic but not in white light. Furthermore, we demonstrated similar AS changes upon light exposure and exogenous sugar supply, with a critical involvement of kinase signaling. We propose that AS is an

integration point of signaling pathways that sense and transmit information regarding the energy availability in plants.

Introduction

Photosynthetic organisms use light as a source of energy, which perpetually fluctuates under natural conditions due to the day-night rhythm, seasonal variation, and non-periodic changes depending on diverse environmental factors. Thus, sensing light and triggering adequate responses is of utmost importance for the survival and reproductive success of photoautotrophs. Plants have evolved complex light signaling mechanisms to adjust numerous aspects of their physiology and development (Jiao et al., 2007; Franklin and Quail, 2010; Kami et al., 2010; Galvao and Fankhauser, 2015), including seedling germination, de-etiolation of dark-grown seedlings, entrainment of the circadian clock, chloroplast movement, stomatal opening, phototropism, shade avoidance, and the timing of flowering.

Higher plants possess at least five classes of photoreceptors mediating responses to different light qualities: red and far-red light can be sensed by phytochromes (PHYs) (Bae and Choi, 2008), blue and ultraviolet-A (UV-A) radiation are mainly detected by cryptochromes (CRYs, Lin and Shalitin, 2003), phototropins (Briggs and Christie, 2002) as well as members of the ZEITLUPE family (Somers et al., 2000; Imaizumi et al., 2003), while UV-B light is detected by the receptor UVR8 (Rizzini et al., 2011; Heijde and Ulm, 2012). Many of the light-regulated processes are responsive to different light qualities and photoreceptor types, and require integration with additional signaling pathways determining plant development and adaptation. Further information on the light status is perceived in the chloroplast by means of photosynthesis, which has been demonstrated to regulate gene expression in different compartments, including retrograde signaling from the plastid to the nucleus (Foyer et al., 2012). Importantly, retrograde and photoreceptor-mediated signaling are interconnected to enable a coordinated response (Ruckle and Larkin, 2009; Estavillo et al., 2011; Lepisto and Rintamaki, 2012; Ruckle et al., 2012).

Plant adaptation to altered light conditions can result in massive changes in plant physiology and growth, e.g., de-etiolation of dark-grown seedlings entails reduced hypocotyl elongation, opening of the apical hook, and both expansion and greening of the cotyledons (Franklin and Quail, 2010; Kami et al., 2010). The molecular mechanisms underlying these phenotypic adaptations have been intensively studied,

revealing complex light-regulated transcriptional networks (Jiao et al., 2007) as well as other modes of gene activity control. Major aspects of light signaling occur within the nucleus, into which PHYs are translocated upon light activation (Nagatani, 2004). However, light signaling has also been shown to include translational control in the cytosol (Liu et al., 2012b; Paik et al., 2012).

Early steps in light signaling include inactivation of negative regulators such as PHYTOCHROME INTERACTING FACTORS (PIFs; Duek and Fankhauser, 2005; Monte et al., 2007), DE-ETIOLATED 1 (DET1), and CONSTITUTIVE PHOTOMORPHOGENIC 1 (COP1; Lau and Deng, 2012). Subsequently, photomorphogenesis-promoting transcription factors are expressed, resulting in the activation of downstream transcriptional networks (Hoecker, 2005; Bae and Choi, 2008). Furthermore, light signaling can alter histone marks and change chromatin organization (van Zanten et al., 2010; Fisher and Franklin, 2011). Light-induced switching from skoto- to photomorphogenesis is accompanied by fundamentally altered gene expression patterns. For instance, more than 20% of all genes in rice and *Arabidopsis thaliana* are differentially expressed in dark-grown compared to light-exposed seedlings (Ma et al., 2001; Tepperman et al., 2001; Jiao et al., 2005; Jiao et al., 2007).

Earlier studies mainly considered quantitative changes in gene expression upon altered light signaling. However, it is now becoming evident that alternative precursor mRNA (pre-mRNA) processing substantially increases transcriptome complexity and can play an important role in modulating gene expression in response to internal and external cues. Among these mechanisms, alternative pre-mRNA splicing (AS) is particularly widespread in higher eukaryotes including plants, affecting more than 60% of all intron-containing genes in *A. thaliana* (Filichkin et al., 2010; Marquez et al., 2012). While regulation and functions of most AS events remain to be addressed, compelling evidence for the relevance of selected AS instances in plant physiological responses has been provided (Syed et al., 2012; Reddy et al., 2013; Staiger and Brown, 2013). For example, intricate links between the circadian clock and AS regulation were uncovered in *A. thaliana* (Sanchez et al., 2010; Staiger and Green, 2011; James et al., 2012; Wang et al., 2012).

AS is perfectly suited to coordinately regulate gene expression, and might play an important role in plant light signaling as well. This hypothesis is supported by the

functional analysis of selected AS events, and previously described effects of light conditions on AS in different plant species. For the PHY-specific type 5 phosphatase, two protein variants with distinct sub-cellular localization patterns are derived from AS of the corresponding pre-mRNA (de la Fuente van Bentem et al., 2003). In the case of a homolog of the light-regulatory transcription factor LONG HYPOCOTYL 5 (HY5), HY5-HOMOLOG (HYH), AS generates transcript variants encoding protein versions with different stabilities (Sibout et al., 2006). However, the regulation of these AS events and their putative role in light signaling were not investigated. Examples for the influence of light conditions on AS include genes encoding an ascorbate peroxidase (Mano et al., 1997) as well as a hydroxypyruvate reductase (Mano et al., 1999) in *Cucurbita sp.* (pumpkin), and high-light-modulated AS for homologs of the family of serine/arginine-rich (SR) splicing factors from *A. thaliana* (Tanabe et al., 2007). Comparisons of AS profiles for light- versus dark-grown rice seedlings using microarrays (Jung et al., 2009) and for *A. thaliana* seedlings with a high-resolution reverse transcription polymerase chain reaction (RT-PCR) panel (Simpson et al., 2008) indicated that light-mediated changes in AS patterns might affect the expression of numerous genes. This notion was further supported by recent studies using RNA sequencing (RNA-seq) to deduce light-regulated AS patterns in a transcriptome-wide manner in the moss *Physcomitrella patens* (Wu et al., 2014), etiolated *A. thaliana* seedlings (Shikata et al., 2014), and light-grown *A. thaliana* plants (Mancini et al., 2016). Interestingly, Wu et al. (2014) and Shikata et al. (2014) reported PHY signaling acting upstream of light-regulated AS. By contrast, AS patterns for a subset of genes in *A. thaliana* exposed to alternating light/dark conditions changed independent of photoreceptors (Petrillo et al., 2014a; Petrillo et al., 2014b; Mancini et al., 2016). These findings raise the intriguing questions whether independent signaling pathways in light-regulated AS exist and how AS changes can contribute to plant adaptation to altered light conditions. The identification of the SR-like splicing factor REDUCED RED-LIGHT RESPONSES IN CRY1CRY2 BACKGROUND 1 (RRC1) as a novel component of PHYB signaling uncovered a further connection between light signaling and AS (Shikata et al., 2012a; Shikata et al., 2012b). The *rrc1* mutant was impaired in the PHYB-dependent light response and showed AS changes for several SR genes (Shikata et al., 2012b). RRC1 functioning in light signaling was dependent on its C-terminal arginine/serine-rich (RS) region (Shikata et al., 2012a). Given that the RS domain of splicing factors

is assumed to play an important role in spliceosome assembly (Reddy et al., 2013), it can be anticipated that RRC1 acts in PHYB signaling via light-regulated AS of downstream targets.

In this work, we analyzed transcriptome-wide gene expression and AS changes in etiolated *A. thaliana* seedlings exposed to blue, red, and white light. Our study revealed that light signals trigger rapid AS responses of numerous genes, including splicing factors and other functional groups. Among these candidates was *RRC1*, which was previously shown to play a role in PHYB signaling. The light signaling phenotype of an *rrc1* mutant could only be complemented with the splicing variant that is up-regulated upon light exposure, indicating the presence of a self-reinforcing circuit. Based on AS analyses under different light conditions, the major photoreceptors for blue and red light play no essential role in regulating these events during photomorphogenesis in white light. Interestingly, the AS output was similarly changed by light and sugar feeding in darkness, and depended on kinase signaling. Our data also revealed a correlation between the AS output and expression of target genes of SUCROSE-NON-FERMENTATION1-RELATED KINASE 1, a central integrator of plant energy signaling.

Results

Dark-grown seedlings display numerous alternative splicing changes upon exposure to blue, red, or white light

Previous studies have established massive transcriptomic re-programming in the switch from skoto- to photomorphogenesis (Jiao et al., 2007). To investigate the potential impact of AS on gene expression in response to altered light conditions, we analyzed transcriptomes of *A. thaliana* seedlings grown for 6 days in darkness and exposed for 1 or 6 h to blue, red, or white light by RNA-seq. Two replicate samples for each time point and light quality, as well as corresponding dark controls were generated. Mapping of the 100-bp-reads to the *A. thaliana* genome (TAIR10 annotation) resulted in 86.0 - 207.6 x 10^6 reads per time point, based on the two replicate samples each (Supplemental Tab. 1). AS events were extracted from TAIR10 and complemented by unannotated events that were found in our data resulting in 56,270 AS events. To determine quantitative changes in AS and gene

expression, a previously established and validated computational pipeline was applied (Rühl et al., 2012; Drechsel et al., 2013; Drewe et al., 2013, Supplemental Data Set 1 and 2). Upon 1 h exposure to blue (~6 µmol m^{-2} s^{-1}) or red light (~14 µmol m^{-2} s^{-1}) at intensities that, based on previous publications (e.g. Laubinger et al. (2004), Shen et al. (2007)), are expected to result in overall saturating effects on hypocotyl elongation, 81 AS events derived from 51 genes were significantly altered (false discovery rate, FDR < 0.1; this FDR value is generally used unless otherwise mentioned; Supplemental Fig. 1A). The number of AS changes massively increased after 6 h blue or red light illumination (Fig. 1A, B). Additional AS shifts were detected upon exposure to white light (~130 µmol m^{-2} s^{-1}), representing more natural light conditions. Considering all three light settings, 700 AS events associated with 311 genes were significantly altered upon 6 h light exposure. As the rate of change in transcript steady state levels depends on transcript stability, early AS shifts will only be detectable for relatively unstable transcripts. We found only few consistent AS changes when comparing the 1 h and 6 h time points for blue and red light (Supplemental Data Set 1). This limited overlap can be explained by overall weak AS changes at the early time point and the activation of downstream signaling cascades at 6 h versus 1 h light exposure. To investigate the potential role of AS in all of these light-regulatory processes, we focused our further analysis on the 6 h time point. We noticed that the AS responses for the three light qualities showed only a partial overlap, independent of the FDR cutoff value (Supplemental Fig. 1B). While blue and red light primarily elicit CRY and PHY photoreceptor signaling, respectively, both signaling pathways should become active in response to white light. Thus, most of the AS changes observed in response to monochromatic light were also expected to be present upon white light exposure. To reduce the effect of AS fluctuation between samples, which is expected to be most prevalent for low-abundant splicing variants with few supporting reads, and to select for AS events that are more likely biologically relevant, we included an additional filter for effect size (change in splicing index, SI > 0.05; Supplemental Fig. 1C & Supplemental Data Set 3). Addition of the SI filter reduced the number of detected events, while the overlap between the different light qualities was still limited. We assumed that this might be caused by a too stringent FDR filter. Therefore, we considered next all events with an FDR < 0.1 in at least one color, and then filtered for SI > 0.05 (Fig. 1C). Applying this filter strategy resulted in strongly overlapping patterns of AS changes for all three light qualities, with 87.5% -

98.0% of all events altered in one color being also affected in at least one more light condition (Fig. 1C). The majority of AS events were changed under all three light regimes, indicating common AS responses. Red light caused fewer significantly altered events upon FDR filtering and a lower median SI change of 0.079 compared to 0.137 and 0.136 in blue and white light, respectively (Supplemental Data Set 3). Red light thus had an overall weaker effect on AS than blue and white light. Both the occurrence of mostly common AS changes in response to different light qualities and, for some AS events, weaker quantitative effects of red light were confirmed by the validation experiments (see below).

Of all 56,270 AS events detected in this analysis, 46.9%, 22.4%, 21.2%, and 9.5% corresponded to alternative 3' splice sites, regulated introns (varying rate of intron retention/splicing), alternative 5' splice sites, and regulated exons (cassette exons), respectively (Supplemental Fig. 2A). The AS analysis in this work is based on a heuristic method, and it was demonstrated to compare favorably to related approaches (Kahles et al., 2016). Similar frequencies of the different AS types have been observed in previous studies using the same, but also with different AS analysis pipelines, and are also found for the TAIR10 annotation (Supplemental Table 2). According to these data sets, alternative 3' splice sites are most abundant, whereas a previous survey of AS in *A. thaliana* identified intron retention as the prevalent AS type (Marquez et al., 2012). These discrepancies most likely result from using different computational approaches for defining splicing variants, including many low-abundant isoforms that might not be biologically relevant. Indeed, a very different distribution was found for the 700 light-regulated AS events: cassette exons and regulated introns were enriched, representing 18.0% and 37.1%, respectively, of all AS events altered in response to at least one light quality, while lower fractions of alternative 3' (27.3%) and 5' (17.6%) splice sites were observed. Among the light-regulated AS events, we also identified several exitrons (Supplemental Table 3), a class of cryptic introns that reside within the coding region of transcripts (Marquez et al., 2015). Analyzing the direction of the shift for the AS events that were significantly altered in response to at least one light quality, we observed strong biases for the intron retention and cassette exon events (Supplemental Fig. 2B). In 74% of the significantly changed intron retention events, light triggered a shift towards the spliced, i.e., shorter transcript variant, while in 67% of the cassette exons a relative increase of the skipping variant was detected. Proportions of alternative up- and

downstream 5’ and 3’ splice site usage, respectively, were also elevated in response to light, but this effect was less pronounced than for the other two AS types. To assess the potential consequences of light-regulated AS on the expression of the corresponding genes, we compared the positions of all events to those displaying significant changes (Supplemental Figure 2C & Data Set 4A-D). For the light-regulated AS events, the fractions of events associated either with the coding sequence or the 3’ untranslated region (UTR) were decreased and increased, respectively, in comparison to all events. For all subsets, however, most of the AS events overlapped with the coding sequence. Based on their positions within the pre-mRNAs, light-triggered AS events can affect the coding and regulation potential of the resulting mRNAs.

Previous studies have revealed widespread coupling of AS and nonsense-mediated decay (NMD) in *A. thaliana* (Kalyna et al., 2012; Drechsel et al., 2013). To assess the prevalence of coupled AS-NMD in the context of light regulation, the occurrence of NMD-triggering features in the corresponding splicing variants was analyzed. To this end, the AS events were integrated into the representative transcript isoform from TAIR10, followed by the detection of upstream open reading frames (uORFs), premature termination codons (PTCs), and long 3’ UTRs (Supplemental Data Set 4A-D). Remarkably, 77.2% of all light-regulated AS events exhibit NMD features within the splicing isoform that is relatively more abundant in the dark samples. Furthermore, 61.1% of all events showed a relative switch from a putative NMD target to a non-NMD regulated transcript variant upon light exposure. The corresponding fractions were even larger when only considering events within the coding sequence, which accounted for most NMD-triggering features in those transcripts. Further evidence for coupling of light-regulated AS and NMD was provided by comparing the sets of significant events from this study and from a previous analysis upon NMD impairment (Drechsel et al., 2013): ~10% of all light-regulated events have previously been established to involve NMD control (Supplemental Data Set 4E-G). Notably, the seedlings analyzed in this and the previous work substantially differed in their developmental stage and growth conditions. The frequency of coupled AS-NMD was analyzed in light-grown seedlings, while the current study revealed that most of the light-regulated AS-NMD events showed downregulation of the putative NMD form in light. Thus, the overlap might be even higher when analyzing seedlings cultivated under identical conditions.

In conclusion, light-triggered AS typically mediates a switch from a presumably NMD-regulated transcript to a protein-coding alternative variant, enabling the activation of gene expression in the transition from skoto- to photomorphogenesis.

The RNA-seq data were also analyzed for differential gene expression (Anders and Huber, 2010; FDR ≤ 0.1; Supplemental Data Set 2). In line with previous findings (Jiao et al., 2007), a substantial fraction of all genes were significantly up- or down-regulated in response to light (Fig. 1D and Supplemental Fig. 3). Out of 33,602 genes in the TAIR10 annotation, 23,432 genes were expressed in our data set when considering all samples (FDR ≤ 0.1; method based on Gan et al., 2011). Furthermore, 10,271 (43.8%) of the expressed genes showed altered transcript levels in response to at least one light quality for the 6 h time point. White, blue, and red light changed the expression of 9,336, 4,381, and 4,251 genes, respectively. When setting a threshold of an at least two-fold change in transcript levels, 3,439, 2,406, and 2,020 were differentially expressed upon seedling exposure to white, blue, and red light, respectively. This adds up to a total number of 4,310 genes, corresponding to 18.4% of all expressed genes. Patterns of differential gene expression in response to blue and red light showed a huge overlap and most of the changes in transcript levels upon illumination with mononochromatic light were also detected under white light. Furthermore, blue and red light affected the expression of a comparable number of genes, while on the level of AS red light was less effective than blue light. Moreover, many transcriptional changes were only found in response to white light, possibly as part of an adaptive program that is not activated by weak, monochromatic light. When considering differential expression separately for up- and down-regulated genes, slightly more genes were induced than repressed at the 6 h time point. We also analyzed differential gene expression for the samples exposed to light for 1 h (Supplemental Fig. 3). In line with the observations on the level of AS, fewer changes were detected for the 1 h compared to the 6 h time point. For this earlier time point, the number of induced genes was approximately twice the number of downregulated ones. Fewer down- than upregulated genes can not only be explained by a lower number of repressed than induced genes, but also by the stability of the transcripts: a significant decrease in steady state transcript levels as a result of diminished transcription within 1 h is expected to be detectable only for highly unstable transcripts.

To test if light affects both expression levels and AS of genes, the corresponding gene lists were compared separately for white, blue, and red light (Fig. 1E, F; Supplemental Fig. 1D). For all light qualities, a substantial fraction of the genes showing changes in AS had unchanged total transcript levels. Given that AS can contribute to quantitative gene control, for example by generating destabilized NMD targets (Drechsel et al., 2013), the number of light-regulated genes displaying both altered AS and differential gene expression in a splicing-independent manner might be even smaller. In summary, the altered light status triggers complex transcriptome reprogramming, involving changes in both gene expression and, for a smaller, mostly distinct set of genes, AS.

Analyzing the functional categories of genes associated with light-regulated AS revealed an overrepresentation of the terms “RNA” and “metabolism” for blue light and “RNA” for white light (Fig. 1G, Supplemental Data Set 5). The overrepresentation of the “RNA” category is in line with previous publications (e.g. Filichkin et al., 2010; Rühl et al., 2012; Drechsel et al., 2013), showing extensive regulated AS for genes involved in RNA metabolism. Since numerous intergenic regions are expressed in an NMD-regulated manner (Drechsel et al., 2013), we compared read accumulation in intergenic regions for the dark- and light-exposed samples (Supplemental Data Set 6). Several of these transcriptional units were found to overlap with previously identified long intergenic RNAs (Liu et al., 2012a). Read coverage for some of these regions differed substantially between the light conditions tested here. However, total expression levels were low in most cases and further studies are required to test the functional relevance of these transcripts.

Finally, to rule out the occurrence of rhythmic expression in the absence of light, transcript levels of circadian genes were analyzed in the dark and light samples (Supplemental Table 4). When comparing the 0 and 6 h dark samples, no significant change was detectable for any of the genes. By contrast, light altered the expression of several of these genes, in line with the known role of light in influencing circadian expression patterns (Jiao et al., 2007).

Validation of light-regulated AS events

We next selected candidates from the list of light-regulated AS events for an independent experimental validation (Fig. 2). This selection covered different functional categories of genes, including splicing factors (Fig. 2A-D), putative

transcription factors (Fig. 2E-G), and a photosynthetic component (Fig. 2H). All of the candidate events were confirmed, in line with the high validation rate observed in previous studies that applied the same pipeline for AS analysis (Rühl et al., 2012; Drechsel et al., 2013). For some genes, several AS events were detected and we focused our analysis on the major splicing variants, which were also sequenced (Supplemental Fig. 4). For all events, the AS ratios were changed in response to blue, red, and white light. However, the extent of splicing change differed for some candidates (Fig. 2). For those candidates, white light generally caused the strongest AS shifts. Furthermore, for 3 out of 9 candidates, a weaker change in response to red compared to blue and white light was observed. These findings are in agreement with differences in the SI changes for the three light qualities from the RNA-seq data.

Light-Regulated AS of *RRC1* Results in a Self-Enforcing Circuit

Previous work had identified the putative splicing factor RRC1 as a novel component of PHY-dependent light signaling (Shikata et al., 2012b). Interestingly, our RNA-seq data suggested that the inclusion of the third exon of *RRC1* is regulated in a light-dependent manner (Fig. 3A). Analyzing the AS pattern of this region via RT-PCR supported the notion that blue, red, and white light caused a shift toward the inclusion variant compared to dark samples (Fig. 3B). Separate quantitation of the two splicing variants revealed that light exposure resulted in slightly elevated levels of the representative *RRC1.1* variant and diminished amounts of *RRC1.2* (Supplemental Fig. 5A). Opposite changes in the levels of the two splicing variants were also observed for the light-regulated event in *SR30* (Supplemental Fig. 5B), indicating that those shifts in splicing variant ratios are caused by AS and not by an altered transcript turnover rate. The exon skipping variant *RRC1.2* gives rise to a frame-shift, resulting in a PTC two exons further downstream. We therefore assumed that this AS variant is targeted by NMD, which was corroborated by its accumulation in two mutants impaired in NMD activity (Fig. 3C).

To test the functional significance of light-regulated AS of *RRC1*, complementation of the *rrc1-2* mutant, carrying a T-DNA insertion (Fig. 3A) and previously described as a knockdown allele (Shikata et al., 2012b), was performed. Subsequently, we determined hypocotyl lengths of seedlings grown in red light or darkness (Fig. 3D). Median hypocotyl lengths in darkness were similar for all tested lines (Supplemental Fig. 6A) and lengths measured in red light were normalized to the average dark value

for each line to correct for a potential light-independent growth phenotype. In line with the previous report by Shikata et al. (2012b) and the role of RRC1 as a positive regulator of light signaling, *rrc1-2* had longer hypocotyls than the wild type (WT; Fig. 3D). This phenotype could be rescued upon complementation with the splicing variant *RRC1.1*, but not *RRC1.2* under control of the constitutive 35S promoter. Complementation with a corresponding genomic construct also resulted in significantly shorter hypocotyls compared to the *rrc1-2* mutant, even though the median length was still slightly elevated compared to the WT. The differences in hypocotyl lengths when comparing complementation with *RRC1.1* and the genomic construct might be caused by varying levels of overexpression (Supplemental Fig. 6B). Analysis of the *RRC1* levels for the two splicing variants and total transcripts confirmed robust and specific expression of the constructs in all transgenic lines. However, the genomic construct resulted in massive over-accumulation of *RRC1* transcripts compared to a more moderate increase in the cDNA lines. To exclude an effect of using a strong constitutive promoter for the complementation, the constructs based on the two AS variants were also expressed in the WT background. None of these lines displayed altered hypocotyl lengths compared to WT (Supplemental Fig. 6C-E). Moreover, immunoblot analysis allowed the detection of a protein corresponding to the splicing variant *RRC1.1*, but not *RRC1.2* (Supplemental Fig. 6F), further suggesting that the exon skipping variant is subject to NMD and does not lead to RRC1 protein. In line with the transcript data, protein levels were much higher in the plants expressing the genomic construct compared to complementation with the *RRC1.1* construct. The strong over-expression of *RRC1* upon complementation with the genomic construct might result in perturbed downstream signaling, which would explain the only partial rescue of the hypocotyl elongation phenotype in case of this construct. To exclude such effects, the *rrc1-2* mutant was also complemented with constructs under control of the *RRC1* promoter. Indeed, the genomic *RRC1* sequence under control of the endogenous promoter fully rescued the mutant phenotype (Supplemental Fig. 7A, B). Expressing the two *RRC1* splicing variants under control of the endogenous promoter resulted in transcript levels that were substantially lower than in the WT, possibly due to the absence of introns (Supplemental Fig. 7C). Accordingly, functional complementation of the hypocotyl phenotype was found only for the *RRC1.1* line with the highest expression (Supplemental Fig. 7D). As expected, none of the *RRC1.2* lines showed a rescue of

the mutant phenotype. Taken together, light-stimulated inclusion of the cassette exon represents a mechanism to induce functional *RRC1* expression, thereby increasing the levels of a positive regulator of light signaling.

Contribution of Photoreceptors to AS Changes during Photomorphogenesis

Recent studies in *P. patens* (Wu et al., 2014) and etiolated *A. thaliana* seedlings (Shikata et al., 2014) suggested a major role of PHY photoreceptors in red light-dependent AS, whereas altered AS patterns in leaves subjected to varying light conditions were attributed to retrograde signaling (Petrillo et al., 2014b). These seemingly controversial findings may result from different experimental settings and suggest that various factors can influence AS patterns under changing light conditions. To further address this intriguing aspect, we first compared the AS patterns of five confirmed candidates in etiolated WT and *phyA phyB* double mutant seedlings upon illumination with white light (Fig. 4A). For all events, very similar patterns of light-induced AS changes in the comparison of WT and *phyA phyB* mutant seedlings were observed; significant differences between WT and the mutant were only found for single events and time points, and did not correlate with the overall light response. Interestingly, seedling growth on sugar-containing medium, as in the RNA-seq experiment, shifted the AS ratio into the same direction as light (Fig. 4A, right panels). The relative change upon 6 h of light exposure, however, was identical for seedlings grown without and with external sugar supply and also did not differ between WT and *phyA phyB* (Supplemental Fig. 8).

Our data did not provide evidence for a critical role of the two major red light photoreceptors PHYA and PHYB in triggering AS changes upon exposure to white light. Given that white light could trigger AS via red- and blue-light-signaling, we next analyzed changes in AS upon exposure to red light (Fig. 4B, Supplemental Fig. 8). For four out of five events, red light resulted in an AS change in both WT and *phyA phyB* seedlings. Interestingly, the mutant showed a significantly weaker red light response than the WT for *MYBD*. Furthermore, the AS ratio of *PPL1* was not significantly changed in comparison of darkness and red light in the mutant. These data suggested the existence of alternative pathways controlling light-triggered AS, and that a contribution of PHYA/PHYB only becomes detectable for some events under red light. We therefore assumed that exposure of seedlings to far-red light, which triggers PHYA signaling but does not support photosynthesis and the

associated signaling, should result in more distinct AS responses in WT and *phyA phyB* seedlings. Far-red light caused an AS shift of all tested events in the WT, albeit quantitative changes for *SR30* were substantially lower than under white light (Fig. 4C, Supplemental Fig. 8). Remarkably, no or only very weak effects of far-red on the AS pattern in the mutant was detected, revealing the dependency on PHY under this particular light condition.

The differences in AS responses under white, red, and far-red light highlight the occurrence of multiple signaling pathways, and that the major PHYs A and B are not essential in this process under white light. Besides PHY signaling, white light also activates the blue light-responsive cryptochome photoreceptors. To test for a potential role of CRYs, AS changes upon exposure to white light were compared between WT and *cry1 cry2* mutant seedlings. All tested events showed the same white light response in WT and *cry1 cry2* seedlings (Fig. 5A, Supplemental Fig. 8). Overall similar AS changes in WT and *cry1 cry2* seedlings were also detected upon blue light exposure (Fig. 5B). The relative AS changes between darkness and 6 h blue light were slightly more pronounced in the WT than in the mutant (Supplemental Fig. 8); however, this quantitative difference was statistically significant only for *SR30*. Taken together, neither PHYA/B-dependent red light signaling nor CRY-mediated blue light signaling are essential in causing the AS changes in etiolated seedlings exposed to white light. This observation could be explained by alternate signaling through either PHYs or CRYs; in this case, however, no AS changes would be expected upon red and blue light exposure of the *phyA phyB* and *cry1 cry2* mutant, respectively. While a role of other photoreceptor types cannot be fully excluded, it seems more likely that another, photoreceptor-independent signaling pathway is involved in light-responsive AS during photomorphogenesis.

Illumination of etiolated seedlings will not only activate photoreceptor signaling and photosynthesis, but also entrain the expression of circadian regulators. Previous reports revealed intricate links between the circadian clock and AS in plants (Sanchez et al., 2010; James et al., 2012). To address a potential impact of circadian regulators, we tested light-triggered AS in mutants defective in different components of the circadian clock (Supplemental Fig. 9). Only for the *prr7-3 prr9-1* double mutant a slightly weaker AS change was seen in case of *RRC1*, suggesting that overall

circadian regulators do not play a major role in the control of these AS events in the early phase of photomorphogenesis.

AS Output Correlates with the Plant's Energy Supply

Analysis of the light-responsive AS in etiolated seedlings revealed that not only light, but also the growth conditions had a major impact on the splicing outcome. Etiolated seedlings grown on sucrose-containing medium had AS ratios shifted into the same direction as observed for seedlings grown without sucrose and exposed for 6 h to light (Fig. 4, 5). To further dissect how light and sugar can alter AS patterns, WT seedlings grown in darkness and on sugar-free medium were transferred to liquid medium with or without sugar, and kept in darkness or exposed to white light. To account for the osmotic effect of sugar supplementation, an additional control with an equimolar concentration of mannitol was included. No significant change in AS was detected upon 1 h incubation in darkness when comparing medium without supplement, with mannitol, and with sucrose (Fig. 6A). In line with the previous findings, light exposure resulted in a pronounced AS shift already after 1 h of illumination. Interestingly, at the 6 h time point, the sugar-treated and dark-kept seedlings showed a pronounced AS shift in the same direction and of a similar extent as observed in light without sugar supply. For several events, the presence of both sugar and light caused an even stronger AS shift than the single treatments (Supplemental Table 5).

Many of the light-induced AS events are expected to be coupled to NMD. To test if the AS shift under these conditions might be, at least to some extent, a consequence of altered NMD activity, we compared the AS response to light and sucrose in etiolated WT and NMD mutant seedlings. Analysis of three predicted AS-NMD events revealed identical AS shifts in WT and *lba1* seedlings upon exposure to light and sucrose (Supplemental Fig. 10), irrespective of the accumulation of the predicted NMD variant in the *lba1* mutant. These data and the separate quantitation of splicing variants (Supplemental Fig. 5) indicate that the changes occur on the level of AS and not downstream of it.

The strong effect of sucrose feeding on the AS output is in line with a previous study, suggesting that retrograde signaling contributes to AS control in light-grown plants (Petrillo et al., 2014b). Accordingly, light-mediated AS is suppressed in green plants upon chemical inhibition of photosynthesis by DCMU (3-(3,4-Dichlorophenyl)-1,1-

dimethylurea; Petrillo et al., 2014b & Supplemental Fig. 11). Treatment of etiolated seedlings with the same inhibitor also slightly weakened, yet did not completely abolish the AS shift in our study (Supplemental Fig. 11). The weaker suppression of light-mediated AS by DCMU in etiolated seedlings might be explained by the absence of an active photosynthesis apparatus. Indeed, different effects of DCMU on light- and dark-grown plants have been described before (Mancinelli, 1994). Alternatively, upon disruption of photosynthesis, photoreceptor-mediated AS control might become detectable in etiolated seedlings, but not in light-grown plants.

We next tested the effect of different sugars on the AS output. Treatment of etiolated seedlings with sucrose, glucose, or trehalose in the absence or presence of light revealed that sucrose was most effective (Fig. 6B). Exposure to 0.2% sucrose caused a strong AS shift, which was further enhanced in the presence of 2% sucrose (Fig. 6B). Glucose feeding caused a slightly weaker AS shift than sucrose. We also treated seedlings with trehalose to trigger accumulation of trehalose 6-phosphate (Schluepmann et al., 2004), which has previously been described as a signal for carbon availability (Schluepmann et al., 2012); however, trehalose exposure had only a minor effect on the splicing outcome. Based on these findings, we postulate that the AS output might be regulated in response to the plant's energy supply, possibly mediated by the level of sucrose, the major transport form of photoassimilates.

Upstream Signaling Involved in Light- and Sugar-Mediated AS Changes

Both sugar feeding and light-driven photosynthesis alter the plant's energy signaling, which might be an integration point resulting in the AS changes observed here. Independently acting systems for sensing the plant's energy status have been described, including HEXOKINASE 1 (HXK1) and SUCROSE-NON-FERMENTATION1-RELATED KINASE 1 (SnRK1, Sheen, 2014). To test their potential relevance under the conditions of our experiments, transcript levels of *HXK1*, *CHLOROPHYLL A/B BINDING PROTEIN 1* (*CAB1)*, which is known to be induced by light (Brusslan and Tobin, 1992), and the SnRK1 targets *DARK INDUCED (DIN) 1* and *DIN6* were measured in seedlings transferred to control or supplemented media and incubated for 6 h in light or darkness (Fig. 6C, Supplemental Fig. 12). Expression levels of *HXK1* were unaffected by both sugar and light, while *CAB1* transcript levels were elevated only in response to light. *DIN1* and *DIN6* levels, however, correlated with the AS pattern shifts, altering in response to

sugar and light. *DIN1* and *DIN6* transcript levels were reduced in response to light and, to an even greater extent, upon sugar exposure. As for the AS shifts, the maximum effect was visible when both sugar and light were supplied. The light- and sugar-responsive expression patterns of *DIN1* and *DIN6* are in agreement with previous reports (Thum et al., 2003; Baena-Gonzalez et al., 2007).

The resemblance of the AS and DIN expression changes in response to light and sugar application would be in line with a coupling of these processes, which we first tested using a *snrk1.1* mutant. Molecular characterization of the *snrk1.1-3* mutant revealed that the T-DNA insertion resulted in an altered transcript and no detectable SnRK1.1 protein (Supplemental Figs. 13, 14). Comparing the AS patterns in etiolated WT and *snrk1.1-3* seedlings showed a slightly different sugar response in darkness (Supplemental Fig. 15A). However, both the AS and DIN expression responses (Supplemental Fig. 15B) were overall similar in WT and mutant seedlings, suggesting remaining activity of the mutant allele or functional redundancy of the two close homologs SnRK1.1 and SnRK1.2. In line with this notion, previous studies have shown that the *snrk1.1-3* mutant does not have an obvious growth phenotype (Mair et al., 2015), and that plants are impaired in development and stress responses only upon transient knockdown of both SnRK1.1 and SnRK1.2 (Baena-Gonzalez et al., 2007).

Signaling through SnRK1 is dependent on its kinase activity and can be disrupted by treatment with the kinase inhibitor K252a (Baena-Gonzalez et al., 2007). Thus, chemical inhibition of SnRK1 is expected to mimic its inactivation under conditions of increased energy availability. However, it should be noted that K252a has a broad target spectrum, resulting in the inhibition of various kinases, and not exclusively SnRK1. Treatment of etiolated seedlings with K252a in the dark changed the AS ratio for *SR30*, *PPD2*, and *MYBD* as sucrose supply or light exposure did (Fig. 7). Furthermore, in the presence of K252a, the effect of sucrose supply in darkness on the AS ratio of *SR30* and *PPD2* was significantly enhanced compared to the corresponding controls without inhibitor. An additional effect of K252a on the AS ratio was also observed for some of the light-treated samples. In the case of *RRC1* and *PPL1*, K252a treatment changed AS into the opposite direction compared to sucrose and light treatment. These different AS responses could be explained by the involvement of distinct sets of splicing factors and their regulation upon inhibitor

treatment in a SnRK1-dependent and -independent manner, in line with the broad target spectrum of K252a. Thus, generation of a mutant specifically impaired in both SnRK1.1 and SnRK1.2 activities will be needed to test for a direct role of SnRK1 signaling in these splicing pattern changes. Taken together, our data suggest that in plants AS represents an integration point of multiple signaling pathways that are responsive to altered energy availability.

Discussion

Photomorphogenesis Induces Complex Transcriptome Changes on the Levels of Gene Expression and Alternative Splicing

Previous microarray studies revealed that a substantial proportion of the *A. thaliana* genome is expressed in a light-dependent manner (Ma et al., 2001; Tepperman et al., 2001; Jiao et al., 2005; Jiao et al., 2007). Genome-wide profiling based on oligonucleotide microarrays suggested that approximately 20% of all genes from *A. thaliana* and rice are differentially expressed in comparison of seedlings undergoing skoto- or photomorphogenesis (Jiao et al., 2005). In this study, we used RNA-seq to determine transcriptome profiles in the early phase of photomorphogenesis, induced by exposure of etiolated *A. thaliana* seedlings to blue, red, or white light. We found that 18.4% of all expressed genes show an at least twofold increase or decrease of total transcript levels in response to 6 h light exposure for one or several light conditions. Accordingly, the extent of light-modulated gene expression seems to be comparable in the transition phase and upon constant growth in different light regimes. When comparing different light qualities, blue and red light affected similar numbers of genes, with a substantial gene overlap. This observation is in agreement with previous studies showing that only relatively few genes are specifically regulated by monochromatic light (Ma et al., 2001; Jiao et al., 2005). Furthermore, we found that most of the genes showing altered expression upon exposure to blue and red light, but also many additional genes, were responsive to white light. The finding that white light is most effective can be explained by the activation of both blue and red light signaling as well as by the higher intensity of white light, which was used to analyze the seedling response under standard illumination conditions.

Analysis of our RNA-seq data further revealed that the photomorphogenic response is not only accompanied by differential expression of numerous genes but also involves massive AS changes. Illuminating etiolated seedlings for 6 h caused significant changes in 700 AS events under at least one light condition. Upon additional filtering for the effect size, most regulated AS events were altered under all three light conditions. Interestingly, several AS events showed weaker quantitative changes under red light compared to blue and white light. We used intensities of blue and red light that are expected to overall saturate the effect on hypocotyl elongation. However, this does not exclude that stronger and/or additional AS shifts may be detected upon exposure of etiolated seedlings to monochromatic light of higher intensities due to photoreceptor-dependent and -independent signaling. Comparison of the sets of genes displaying light-modulated gene expression and AS highlighted the existence of mostly distinct and few common targets. This overlap might be even lower, considering that many AS variants from *A. thaliana* have been reported to be targeted by NMD (Kalyna et al., 2012; Drechsel et al., 2013). Accordingly, AS shifts affecting the formation of destabilized transcripts are also expected to change total steady state transcript levels.

To test for a role of coupled AS-NMD in light-responsive gene control, we analyzed which types of AS events are affected and whether this has an effect on the presence of NMD-triggering features. Instances of light-regulated AS were enriched for intron retention and cassette exon events, both of which are known to frequently introduce NMD target features (Kalyna et al., 2012; Drechsel et al., 2013). For example, splicing factors from the family of POLYPYRIMIDINE TRACT BINDING PROTEINS, such as PTB1 and PTB2 from *A. thaliana*, activate inclusion of so-called poison exons in their corresponding pre-mRNAs, thereby introducing PTCs and rendering the transcripts sensitive to NMD (Stauffer et al., 2010). The auto- and crossregulatory mechanism allows balancing of gene expression based on coupled AS-NMD and has been frequently observed for splicing factors from animals and plants (Staiger et al., 2003; Lareau et al., 2007; Isken and Maquat, 2008; Schoning et al., 2008; Palusa and Reddy, 2010; Wachter et al., 2012). Regarding the direction of AS changes, the majority of light-regulated cassette exon and intron retention events resulted in skipping and splicing, respectively, upon light exposure. Interestingly, a previous study in *P. patens* showed the opposite effect for intron retention events, i.e., preferential intron retention upon light exposure (Wu et al., 2014).

Based on the predominant AS shifts observed in our study, we anticipated that light exposure reduces the number of transcripts containing NMD-triggering features. Implementing the AS events into the corresponding full-length transcripts further corroborated this assumption: 77.2% of the light-responsive AS events exhibited NMD target features for the splicing variants being relatively more abundant in darkness. Furthermore, 61.1% of the significant events showed a light-dependent relative shift from a splicing variant containing NMD-eliciting features to an mRNA without such characteristics. It will be interesting to test how many of these transcripts are indeed regulated by NMD, and to what extent accumulation of the corresponding proteins is affected by the changes in AS-NMD. Based on the large number of light-regulated AS events affecting the presence of NMD target features, it seems likely that the expression of numerous genes can be restricted by the formation of NMD-regulated splicing variants in darkness, whereas light shifts the AS outcome towards a more stable mRNA and translation into the corresponding factors. The involvement of coupled AS-NMD in light-triggered processes further expands the functions of NMD, which is increasingly recognized as an important regulator of physiological transcripts besides its role in RNA surveillance (Drechsel et al., 2013; Karam et al., 2013; Gloggnitzer et al., 2014; Sureshkumar et al., 2016). Furthermore, alternative strategies for preventing the translation of unproductive transcripts have been described in plants, in particular nuclear retention of intron-containing transcripts (Göhring et al., 2014). Thus, different mechanisms might contribute to the regulation of gene expression by targeting AS variants predominantly produced in etiolated seedlings.

Light-Dependent AS Defines Expression of Splicing Factors and Is Critical for Light Signaling

The genes containing light-dependent AS events showed an overrepresentation of the functional category “RNA”, including several splicing factors. This observation is in line with previous studies showing extensive and regulated AS for the pre-mRNAs of many splicing factors (Reddy and Shad Ali, 2011; Syed et al., 2012; Wachter et al., 2012; Reddy et al., 2013; Staiger and Brown, 2013; Mancini et al., 2016), which allows quantitative gene control by coupling to NMD (see above) but might also increase their functional diversity. Interestingly, among our candidates was RRC1, a putative splicing factor that had previously been identified as a component of PHYB

signaling (Shikata et al., 2012a; Shikata et al., 2012b). We demonstrated in the current work that the corresponding AS event gives rise to one splicing variant that is degraded via NMD, whereas light promotes the formation of the transcript resulting in RRC1 protein. Complementation experiments using an *rrc1* mutant revealed that only the light-induced splicing variant is able to rescue the mutant defect in red light signaling. Accordingly, generation of this PHY signaling component is limited due to coupled AS-NMD in darkness. The light-mediated AS change is expected to allow increased formation of the RRC1 protein, which, because of its function as a positive regulator of PHY signaling, should further enhance the light response. Previous work showed that the C-terminal arginine/serine-rich (RS) domain of RRC1 is required for its function in PHYB signaling (Shikata et al., 2012a; Shikata et al., 2012b). In general, the RS domain of splicing factors is critical for their splicing regulatory activity (Graveley, 2000; Reddy and Shad Ali, 2011). Hypomorphic *rrc1* mutants lacking the RS domain displayed AS changes for several SR genes (Shikata et al., 2012b), indicating that RRC1 might be directly involved in the regulation of these AS events. Future work needs to address whether RRC1 is a key regulator of downstream light-modulated AS events and what the molecular links to red light signaling are. Analyzing the sequence context of light-regulated AS events identified several enriched motifs (Supplemental Table 6), which might serve as binding sites for RRC1 or other splicing factors involved in this process.

Alternative Splicing Is a Converging Point for Processes Affecting Plant Energy Signaling

Our study revealed that AS of numerous genes is altered upon illumination of etiolated seedlings and, in the case of *RRC1*, can modulate light signaling. To gain a better understanding of light-triggered AS, the upstream regulatory components need to be identified. Two recent studies analyzing light-induced AS in *P. patens* (Wu et al., 2014) and etiolated *A. thaliana* seedlings (Shikata et al., 2014) suggested the involvement of PHY photoreceptors. Notably, comparison of AS changes in WT and *phyA phyB* mutants upon exposure to red light actually identified a larger number of PHY-independent than PHY-dependent events (Shikata et al., 2014; see also Supplemental Data Set 7): upon 1 h red light exposure, 1,505 and 1,714 genes were reported to give rise to PHY-dependent and PHY-independent AS events, respectively. An even lower fraction of PHY-dependent AS events were found upon 3

h red light exposure, triggering AS changes in 1,116 and 2,098 genes in a PHY-dependent and PHY-independent manner, respectively. Surprisingly, most of the events defined to be PHY-dependent were changed only after 1 h or 3 h, raising the question of what the functions of numerous, short-lived AS changes might be. Analysis of the data from Shikata et al. (2014) using our pipeline detected far fewer AS changes and an increase in the number of events from the 1 h to the 3 h time point (Supplemental Data Set 7). The latter is expected, as changes in RNA steady state levels are limited by the RNA stability, and as a consequence of downstream signaling. Both the order of magnitude of regulated AS events and an increase in detectable AS changes over time are in agreement with the results from our RNA-seq data. Shikata et al. (2014) defined AS events to be PHY-dependent when the direction of change was identical in the comparison of dark versus light in WT and *phyA phyB* versus WT in light. We used an alternative constraint for calling events PHY-dependent, which is the occurrence of light-induced AS in the WT, but not in the *phyA phyB* mutant. Using this definition and our analysis pipeline, we identified 329 PHY-dependent and 11 PHY-independent AS changes upon 3 h of red light exposure from the RNA-seq data generated by Shikata et al. (2014) (Supplemental Data Set 7). Thus according to our analysis, almost all AS changes detected upon exposure to red light of this intensity are PHY-dependent.

By contrast, light-triggered AS changes in plants grown in light/dark cycles were shown to be independent of photoreceptors (Petrillo et al., 2014b; Mancini et al., 2016). Based on our data, the PHYA/B and CRY photoreceptors also play no major role in AS control during photomorphogenesis in normal light conditions. AS changes in response to white light were identical in WT compared to *phyA phyB* and *cry1 cry2* mutants, which are defective in the major red and blue light receptors, respectively. Analysis of red-light responsive AS for a splicing factor gene in a *phy* quintuple mutant from *A. thaliana* also excluded, at least in light-grown plants, a role of the other PHYs in this process (Mancini et al., 2016). We observed that a contribution of PHYA/B to light-mediated AS is only detectable under red and far-red light. For most candidates, AS changes in response to red light were less pronounced in *phyA phyB* than in the WT. Similarly, blue light induced slightly weaker AS shifts in *cry1 cry2* compared to WT, albeit this difference was not statistically significant for most events. An even weaker or no AS shift in *phyA phyB* seedlings exposed to red light was shown in the validation experiments from Shikata et al. (2014). Moreover, our

analysis of the RNA-seq data from Shikata et al. (2014) revealed that 97% of the AS changes in red light are PHY-dependent (see above). The varying degree of PHY-mediated AS control upon exposure to red light can most likely be attributed to the use of different light intensities, as 8.3 and ~28 µmol m^{-2} s^{-1} red light, respectively, were used by Shikata et al. (2014) and in our corresponding downstream analyses. Higher intensities of red light might result in an increased PHY response, but also enhance PHY-independent signaling. Accordingly, a stronger activation of photosynthesis at higher light intensities might explain the reduced PHY-dependency of the AS changes under this condition. Furthermore, we found that in response to far-red light, most AS events were unchanged in the *phyA phyB* mutant, while WT seedlings showed similar AS shifts as under white light. Taken together, our data suggest that PHYs and presumably also CRYs can induce AS changes; however, this effect becomes detectable only in artificial monochromatic light conditions. Accordingly, alternative signaling routes must exist and are active under more natural, white light conditions, outweighing the effect photoreceptors have on AS.

Based on our findings, we propose that AS changes during photomorphogenesis in regular light conditions are primarily controlled by a metabolic signal that is derived from photosynthesis. A major role of PHYA/B and CRY photoreceptors only becomes visible under light conditions that do not, or only to a minor extent, support photosynthesis, namely far-red light and relatively weak red light. Moreover, sugar feeding in darkness had a similar effect on the splicing patterns as light exposure. In line with our findings for etiolated seedlings, AS changes in light-grown plants were reported to depend on retrograde signaling from the chloroplast to the nucleus (Petrillo et al., 2014b). In contrast to light-grown plants, etiolated seedlings do not possess a fully developed photosynthesis system. This raises the question of how much time etiolated seedlings need to set up photosynthesis and thereby alter metabolic signaling. While we are not aware of studies reporting the onset of photosynthesis in *A. thaliana* seedlings undergoing photomorphogenesis, former reports on other plant species suggested that photochemical activity of the photosystems is already detectable a few minutes after illumination of etiolated seedlings (Baker and Butler, 1976). In *Hordeum vulgare* (barley), the first CO_2 assimilates were detected 1 h after light exposure (Biggins and Park, 1966). Accordingly, we assume that photosynthesis is activated within the first hours of light exposure, resulting in altered metabolic signaling and changing AS patterns.

Interestingly, previous studies described metabolic repression of photoreceptor signaling (Sheen, 1990; Harter et al., 1993; Dijkwel et al., 1997), which might further limit the role of photoreceptors in the light regulation of AS under photosynthesis-competent conditions. The cross-talk between carbon and light signaling can also substantially change during plant development, as reported for the sugar- and light-responsive transcript levels of three genes in etiolated seedlings compared to light-grown plants (Thum et al., 2003). Similarly, the contribution of different signaling pathways in light-mediated AS might be altered during photomorphogenesis.

Testing the effect of different sugars, we observed that exogenous supply of sucrose caused the most pronounced AS shifts. Exposure of etiolated seedlings to both light and sugar resulted in even stronger AS shifts than the single treatments for most events. This finding can be explained by the existence of independent signaling pathways. Alternatively, the single treatments may not have resulted in saturated responses, e.g. as a consequence of limited photosynthesis or inefficient sugar uptake and transport in the seedlings. Taking into account that already the single treatments resulted in very pronounced AS changes for most candidates, further work will need to examine whether an even stronger AS shift is of functional relevance. At least some of the AS events might allow a gradual response due to the integration of multiple signaling pathways.

Furthermore, we demonstrated that the AS patterns correlated with the expression of *DIN* genes, which are targets of SnRK1, a central integrator of energy and stress signaling (Sheen, 2014). Previous work revealed inactivation of SnRK1 under conditions of high energy availability, in particular under light or upon sugar feeding in darkness (Baena-Gonzalez et al., 2007; Sheen, 2014). Interestingly, we found for several genes that chemical inhibition of kinases caused similar AS shifts as supply of light or sugar, suggesting an important role of phosphorylation in the upstream signaling. However, as the kinase inhibitor used in our study is not specific for SnRK1 and because of the probable functional redundancy of SnRK1.1 and SnRK1.2, further work will be required to test a direct link between SnRK1 signaling and light-/sugar-triggered AS changes. Notably, a role of AS in sugar responses is also supported by the findings that the splicing factor SR45 negatively regulates glucose signaling (Carvalho et al., 2010) and modulates SnRK1 protein stability in *A. thaliana* (Carvalho et al., 2016). SnRK1-mediated metabolic adjustment has been described

to involve direct phosphorylation of key enzymes in metabolism (Sugden et al., 1999; Harthill et al., 2006) and differential transcriptional programs (Polge and Thomas, 2007; Baena-Gonzalez and Sheen, 2008; Mair et al., 2015). Based on our findings, changes in the AS program, mediated through SnRK1 and/or other kinases, might provide an additional and powerful means to adjust metabolism to the plant energy supply.

Methods

Plant cultivation and experiments

Generally, seeds were sterilized in 3.75% NaClO and 0.01% Triton X-100 and plated on ½ MS medium containing 0.8% phytoagar (Duchefa) with or without 2% sucrose added. Sucrose-containing medium was used for the RNA-seq and validation (Fig. 2, 3) experiments. The experiments with the photoreceptor mutants (Fig. 4, 5) were performed in parallel with seedlings grown on medium with and without sugar as indicated. Seeds were stratified for at least 2 days at 4°C, then germination was induced in white light for 2 h. Seedlings were grown in darkness for 6 days and then exposed to white, red, blue, or far-red light, or kept in darkness for the indicated period. Darkness samples were taken in green light.

For hypocotyl assays, seeds were plated singly on plates without sucrose. After the initial 2 h light exposure, plates were placed in red light or in darkness for 6 days. The lines to be compared were grown on the same plates. Seeds were the same age. Seedlings were scanned after transfer to ½ MS plates with 1.5% agar. The length of scanned seedlings was measured using ImageJ (Schneider et al., 2012). All relative hypocotyl lengths are normalized to the average length of each line grown in darkness.

For transfer experiments and sugar treatments (Fig. 6, 7), seeds were plated densely on medium without sucrose and grown in darkness for 6 days after initial light exposure. Seedlings were transferred to liquid ½ MS medium without or with sugar supplementation under green light and incubated in white light or darkness for the indicated periods. For kinase inhibition, 4 µM K252a (dissolved in DMSO) was added; the corresponding mock sample was treated with DMSO only.

For DCMU treatment, light-grown seedlings were cultivated under long-day conditions in white light for 6 days on sucrose-free ½ MS plates. Subsequently, seedlings were transferred to 100 µM DCMU (3-(3,4-Dichlorophenyl)-1,1-dimethylurea; stock dissolved in ethanol, EtOH) or mock solution containing an equivalent concentration of EtOH, followed by 6 h incubation in darkness or white light. Etiolated seedlings were grown for 6 days in liquid medium (½ MS without sucrose) and darkness, followed by DCMU or mock treatment as described for the light-grown seedlings.

The following lines have been used in different experiments: *rrc1-2* (SALK_121526C, N667179), *lba1* (Yoine et al., 2006), *upf3-1* (SALK_025175), *lhy-null* (Yakir et al., 2009), *toc1-101* (Kikis et al., 2005), *prr7-3 prr9-1* (Farre et al., 2005)*, phyA-211 phyB-9 (phyA phyB), cry1-304 cry2-1 (cry1 cry2)*, and *snrk1.1-3* (GABI_579E09; Mair et al., 2015).

Light conditions

Continuous white light had an intensity of ~130 µmol m^{-2} s^{-1}. For monochromatic light LED fields (Flora LED, CLF Plant Climatics) were used. Specifications: blue 420-550 nm, maximum (max) 463 nm, Full Width at Half Maximum (FWHM) 22.2 nm; far-red 680-790 nm, max 742 nm, FWHM 23.8 nm; red 620-730 nm, max 671 nm, FWHM 25 nm. Light intensities are provided in figure legends and have been measured with a Skye SKR1850, using the far-red channel for far-red, and photosynthetically active radiation for blue, red, and white light. Red light intensity of ~10 µmol m^{-2} s^{-1} for hypocotyl assays were achieved by stacking plates with a layer of white paper between them.

RNA-seq analyses

Seedlings were grown in darkness for 6 days, then sampled (0h), or exposed to light for 1 h or 6 h, or kept in darkness for 6 h before sampling (6D). RNA was extracted using the EURx GeneMATRIX Universal RNA Purification Kit. Starting from 4 µg total RNA, libraries were prepared using the Illumina TruSeq Kit v2, Box A mostly according to the manufacturer's instructions (Sample Preparation v2 Guide September 2012). The PCR step was performed using only half the template in a

reaction volume of 34 µL, and the libraries were subsequently purified on a 2% agarose gel. After cutting a band of appropriate size from the gel for each library, the DNA was extracted using the Qiagen MinElute Gel Extraction Kit. Concentrations were determined using the Agilent 2100 Bioanalyzer with the DNA1000 Kit. RNA-seq libraries were prepared using the Illumina TruSeq Kit and sequenced single end with 101 bp read length and a 7 bp index read on the HiSEQ2000, equipped with on-instrument HCS version1.5.15 and Real time analysis (RTA) version1.13. Cluster generation was performed on a cBot (recipe: SR_Amp_Lin_Block_Hyb_v8.0, Illumina) using a flow cell v3 and reagents from TruSeq SR Cluster Kits v3 (Illumina) according to the manufacturer's instructions. The final library DNA concentration was 7 to 8 pM on the flow cell. Samples were duplexed or quadruplexed using the adapters 012, 006, 019, and 005 (see Supplemental Table 1). Each sample was run in biological duplicates.

We used a previously established pipeline for alignment, splice event calling, and analyses (Rühl et al., 2012; Drechsel et al., 2013). In short, RNA-seq reads were aligned to the TAIR 10 reference genome using PALMapper (Jean et al., 2010) in two steps. First, an alignment was performed to discover novel splice junctions. Second, the novel splice junctions were included in the alignment to obtain a splice-sensitive alignment. Subsequently, novel splice events were called using SplAdder (Kahles et al., 2016), as also described in Drechsel et al. (2013). Read counts and differential AS events were determined using rDiff (Drewe et al., 2013). Differential gene expression was analyzed using DESeq (Anders and Huber, 2010). For a detailed description of parameter settings, see Computational Parameter Settings in the Supplemental Method section. To estimate the biological variance and thus determine accurate false discovery rates, the analyses of differential AS events and differential gene expression were performed jointly on all replicates of the samples that were to be compared.

For filtering the results, AS events with an FDR value below a certain threshold were required to not show changes in the opposite direction in any other light condition (i.e. (B_up < FDR and R_down > FDR and W_down > FDR) or (B_down < FDR and R_up > FDR and W_up > FDR) for events changing significantly in blue light). Data analysis was done using Excel (Microsoft) or Python (Anaconda distribution 2.1.0, Continuum Analytics) with SciPy (Jones et al., 2001), NumPy (van der Walt et al.,

2011), Pandas (McKinney, 2010), Matplotlib (Hunter, 2007), and IPython (Pérez and Granger, 2007), or DataJoint (Yatsenko et al., 2015).

Functional clustering using the MapMan software (Thimm et al., 2004) was done as previously described (Rühl et al., 2012; Drechsel et al., 2013), and as detailed in Supplemental Data Set 5. Extraction of NMD features and analysis of intergenic regions were performed as described in Drechsel et al. (2013).

The RNA-seq data described in Shikata et al. (2014) were kindly provided by Kousuke Hanada. Trimming was performed as described in Shikata et al. (2014). Subsequently, the data was analyzed as described for our RNA-seq data. In our analysis of the data described in Shikata et al. (2014), we considered both read ends of the paired-end reads as two independent single-end reads.

Calculation of splicing index and event filtering

For determination of effect sizes, the splicing index (SI) was calculated for each event and light condition. SI is the ratio of the number of spliced alignments supporting the longer isoform, divided by all spliced alignments corresponding to this event. In case of intron retention events, the SI was determined as the average intron coverage divided by the average intron coverage plus the spliced alignments spanning the respective intron. As the reliability of the SI depends on the number of available alignments, no SI index was calculated when fewer than 10 isoform-specific reads were available. SI values for an event of the category ‘old’ were only computed when the event could be confirmed in the respective read library, that is there was a sufficient number of alignments present in the new libraries to call the event.

For comparison of SI values of significantly changed AS events, the following filters were applied: all relevant replicates need to be assigned an SI value, and the variation in SI between replicates needs to be less than 0.25. Furthermore, to exclude splicing variants of low abundance or with minor changes, only those events with SI changes greater than 0.05 were considered as having changed between dark and light samples. When combining data from different light qualities, events with opposite changes in SI > 0.05 were excluded.

RNA extraction, RT, qPCR, and PCR product analyses

RNA was extracted using the Universal RNA Purification Kit (EURx) with an on-column DNase digest as instructed by the manufacturer. Reverse transcription was done with RevertAid Premium (Thermo Fisher), or using AMV Reverse Transcriptase Native (EURx) for light-grown sets of WT and NMD mutant seedlings. The maximum volume of RNA template possible and a dT_{20} primer were used following the manufacturers' instructions.

RT-qPCRs were performed as described previously (Stauffer et al., 2010). In short, the Biorad CFX384 real-time PCR system and MESA GREEN qPCR Mastermix Plus (Eurogentec) were used. *PP2A* (*AT1G13320*) transcript levels were measured for normalization.

RT-PCR fragments were separated and visualized on ethidium bromide stained agarose or polyacrylamide gels. Isoform concentrations were measured using the Agilent 2100 Bioanalyzer with the DNA1000 Kit. Oligonucleotides used are listed in Supplemental Table 7. Gel pictures were enhanced using the Adobe Photoshop autocontrast function.

Splice variants were subcloned using the pGEM-T Vector System I (Promega) or StrataClone PCR Cloning Kit (Agilent) and sequenced, or sequenced directly.

Statistical analysis

Number of biological replicates (n), types of error bars, and statistical analyses are defined in the figure legends.

Cloning procedures

RRC1 overexpression constructs are based on the vector pGWB612 (Nakamura et al., 2010). Oligonucleotide sequences are listed in Supplemental Table 7. CDS of the splicing variants, with the 3' UTR included were amplified from cDNA and the genomic sequence of *RRC1* was amplified from genomic DNA using primers 22/23 and recombined using the Gateway system (Invitrogen) into pDONR207, after PCR extension of the attachment sites with primers 24/25. Subsequently, *RRC1* sequences were recombined into pGWB612. For the complementation constructs under control of the endogenous promoter, an *RRC1* 1013 bp putative promoter fragment including the 5' UTR was amplified using primers 26/27 and exchanged with

the 35S promoter of pGWB612 using *Hind*III/*Xba*I. Subsequently, the cDNA or genomic sequence was introduced as for the overexpression constructs.

Plant transformation

A. thaliana plants were stably transformed by the floral dip method (Clough and Bent, 1998).

Protein extraction and immunoblot analyses

For immunoblot analyses, proteins were extracted as described previously (Rühl et al., 2012), using the following buffers: RRC1 protein was extracted using a denaturing buffer as previously described (Shikata et al., 2012b) with Complete (Roche) as protease inhibitor. SnRK1.1 protein was extracted using 50 mM Tris-HCl (pH 7.5), 150 mM NaCl, 0.1% (v/v) Tween 20, and 0.1% (v/v) β-mercaptoethanol. All extracts were cleared by centrifugation for ~20 min at 15,000 xg and 4°C. SDS-PAGE and semi-dry immunoblotting were performed according to standard protocols. For detection, the following commercial antibodies were used: mouse α-HA (Sigma), rabbit α-SnRK1.1 (Agrisera), α-mouse-peroxidase (Sigma), α-rabbit-peroxidase (Sigma). Chemiluminescence detection used Super Signal West Dura (Pierce).

Data Access

Visualization of RNA-seq data is available at http://gbrowse.cbio.mskcc.org/gb/gbrowse/r403PAS/

Accession Numbers

RNA-seq data have been deposited in the Gene Expression Omnibus repository (http://www.ncbi.nlm.nih.gov/geo) under accession number GSE70575. A list of all analyzed genes is provided in Supplemental Data Sets 1 and 2.

Supplemental Data

Supplemental Data Sets 1-7 are available at http://datadryad.org/resource/doi:10.5061/dryad4nt0f

Supplemental Figure 1. Light-Triggered AS Changes Using Different Filter Criteria.

Supplemental Figure 2. Properties of AS Events.

Supplemental Figure 3. Light-Dependent Changes in Total Transcript Levels.

Supplemental Figure 4. Sequences of Splicing Variants Identified.

Supplemental Figure 5. Changes in Splicing Variant Levels of *RRC1* and *SR30* in Response to White, Blue, and Red Light.

Supplemental Figure 6. Overexpression of *RRC1* Does Not Affect Hypocotyl Length.

Supplemental Figure 7. Complementation of the *rrc1-2* Mutant Using Constructs under Control of the Endogenous Promoter.

Supplemental Figure 8. AS Shifts in Response to White Light Are Comparable in Wild Type and Photoreceptor Mutants.

Supplemental Figure 9. Circadian Regulators Do Not Majorly Influence Light-Dependent AS of Select Candidates.

Supplemental Figure 10. Light- and Sucrose-Triggered AS Changes Are Comparable in WT and NMD Mutant Seedlings.

Supplemental Figure 11. DCMU Treatment Reduces Light-Dependent AS Changes in Light- and Dark-Grown Arabidopsis Seedlings.

Supplemental Figure 12. Transcript Levels of *HXK1* and *CAB1* in Response to Sucrose and Light.

Supplemental Figure 13. Analysis of the T-DNA Insertion Mutant *snrk1.1-3*.

Supplemental Figure 14. Genomic, Transcript, and Protein Sequences for the Wild Type *SnRK1.1* and the Mutant *snrk1.1-3* Alleles.

Supplemental Figure 15. AS Patterns and *DIN* Expression in the *snrk1.1-3* Mutant.

Supplemental Table 1. Alignment Statistics for RNA-seq Data.

Supplemental Table 2. Frequencies of AS Types in Different Datasets.

Supplemental Table 3. Light-Regulated AS Events of "Exitron" Type.

Supplemental Table 4. Genes Underlying Circadian Regulation Are Not Differentially Expressed in Darkness.

Supplemental Table 5. Statistical Comparison of AS Changes in Response to Light and Sugar.

Supplemental Table 6. Motifs Enriched in Light-Regulated AS Events.

Supplemental Table 7. Sequences of DNA Oligonucleotides.

Supplemental Methods. Computational Parameter Settings.

Supplemental Data Set 1. Computational Analysis of Transcriptome-Wide AS.

Supplemental Data Set 2. Computational Analysis of Transcriptome-Wide Differential Gene Expression.

Supplemental Data Set 3. Splicing Index Analysis.

Supplemental Data Set 4. Analysis of NMD Target Features and Overlap between NMD- and Light-Regulated AS.

Supplemental Data Set 5. Categorization of Light-Regulated and Reference Gene Sets into Functional Subgroups.

Supplemental Data Set 6. Expressed Intergenic Regions.

Supplemental Data Set 7. Computational Analysis of Transcriptome-Wide AS changes in response to red light based on the data from Shikata et al. (2014).

Acknowledgments

The authors are grateful to Christa Lanz, Jens Riexinger, and the Genome Center (Max Planck Institute for Developmental Biology) for performing the Illumina sequencing and to Vipin T. Sreedharan for visualization of the RNA-seq data in

GBrowse. We thank the Nottingham Arabidopsis Stock Centre for providing seeds of the *rrc1*, *lba1*, and *upf3* mutants described in this work. Seeds of the *phyA phyB* and *cry1 cry2* mutants were provided by Andreas Hiltbrunner; circadian mutants were received from Hugh G. Nimmo and Allan James, and the *snrk1.1-3* mutant was provided by Elena Baena-Gonzalez. We also thank Gabriele Drechsel for help with MapMan, Anja Possart and Virtudes Mira-Rodado for help with the LED fields, Natalie Faiss for technical support, and Andreas Hiltbrunner, Sascha Laubinger and Klaus Harter for discussion of our findings. Furthermore, we thank the central facilities of the Center for Plant Molecular Biology (University of Tübingen), the Max Planck Society, the Memorial Sloan Kettering Cancer Center, and the ETH Zürich. This work was supported by the German Research Foundation (DFG): WA 2167/4-1, SFB#1101, TP C03, and a Heisenberg fellowship (WA 2167/8-1) to A.W., and RA1894/2-1 to G.R., and by Memorial Sloan Kettering Cancer Center and ETH Zürich to G.R.

Author Contributions

L.H., P.D., G.R., and A.W. designed research; L.H., T.W., G.W., S.G., H.L., D.O. performed experiments; P.D., A.K., J.B., L.H., F.H.S. performed computational analyses; A.W., L.H. wrote the manuscript; all authors contributed to data analysis and discussion.

References

Anders, S., and Huber, W. (2010). Differential expression analysis for sequence count data. Genome biology 11, R106.

Bae, G., and Choi, G. (2008). Decoding of light signals by plant phytochromes and their interacting proteins. Annu Rev Plant Biol 59, 281-311.

Baena-Gonzalez, E., and Sheen, J. (2008). Convergent energy and stress signaling. Trends in plant science 13, 474-482.

Baena-Gonzalez, E., Rolland, F., Thevelein, J.M., and Sheen, J. (2007). A central integrator of transcription networks in plant stress and energy signalling. Nature 448, 938-942.

Baker, N.R., and Butler, W.L. (1976). Development of the Primary Photochemical Apparatus of Photosynthesis during Greening of Etiolated Bean Leaves. Plant physiology 58, 526-529.

Biggins, J., and Park, R.B. (1966). CO(2) Assimilation by Etiolated Hordeum vulgare Seedlings during the Onset of Photosynthesis. Plant physiology 41, 115-118.

Briggs, W.R., and Christie, J.M. (2002). Phototropins 1 and 2: versatile plant blue-light receptors. Trends in plant science 7, 204-210.
Brusslan, J.A., and Tobin, E.M. (1992). Light-independent developmental regulation of cab gene expression in Arabidopsis thaliana seedlings. Proc Natl Acad Sci U S A 89, 7791-7795.
Carvalho, R.F., Carvalho, S.D., and Duque, P. (2010). The plant-specific SR45 protein negatively regulates glucose and ABA signaling during early seedling development in Arabidopsis. Plant physiology 154, 772-783.
Carvalho, R.F., Szakonyi, D., Simpson, C.G., Barbosa, I.C., Brown, J.W., Baena-Gonzalez, E., and Duque, P. (2016). The Arabidopsis SR45 Splicing Factor, a Negative Regulator of Sugar Signaling, Modulates SNF1-Related Protein Kinase 1 Stability. Plant Cell 28, 1910-1925.
Clough, S.J., and Bent, A.F. (1998). Floral dip: a simplified method for Agrobacterium-mediated transformation of Arabidopsis thaliana. Plant J 16, 735-743.
de la Fuente van Bentem, S., Vossen, J.H., Vermeer, J.E., de Vroomen, M.J., Gadella, T.W., Jr., Haring, M.A., and Cornelissen, B.J. (2003). The subcellular localization of plant protein phosphatase 5 isoforms is determined by alternative splicing. Plant physiology 133, 702-712.
Dijkwel, P.P., Huijser, C., Weisbeek, P.J., Chua, N.H., and Smeekens, S.C. (1997). Sucrose control of phytochrome A signaling in Arabidopsis. Plant Cell 9, 583-595.
Drechsel, G., Kahles, A., Kesarwani, A.K., Stauffer, E., Behr, J., Drewe, P., Rätsch, G., and Wachter, A. (2013). Nonsense-mediated decay of alternative precursor mRNA splicing variants is a major determinant of the Arabidopsis steady state transcriptome. Plant Cell 25, 3726-3742.
Drewe, P., Stegle, O., Hartmann, L., Kahles, A., Bohnert, R., Wachter, A., Borgwardt, K., and Rätsch, G. (2013). Accurate detection of differential RNA processing. Nucleic acids research 41, 5189-5198.
Duek, P.D., and Fankhauser, C. (2005). bHLH class transcription factors take centre stage in phytochrome signalling. Trends in plant science 10, 51-54.
Estavillo, G.M., Crisp, P.A., Pornsiriwong, W., Wirtz, M., Collinge, D., Carrie, C., Giraud, E., Whelan, J., David, P., Javot, H., Brearley, C., Hell, R., Marin, E., and Pogson, B.J. (2011). Evidence for a SAL1-PAP chloroplast retrograde pathway that functions in drought and high light signaling in Arabidopsis. Plant Cell 23, 3992-4012.
Farre, E.M., Harmer, S.L., Harmon, F.G., Yanovsky, M.J., and Kay, S.A. (2005). Overlapping and distinct roles of PRR7 and PRR9 in the Arabidopsis circadian clock. Current biology : CB 15, 47-54.
Filichkin, S.A., Priest, H.D., Givan, S.A., Shen, R., Bryant, D.W., Fox, S.E., Wong, W.K., and Mockler, T.C. (2010). Genome-wide mapping of alternative splicing in Arabidopsis thaliana. Genome Res 20, 45-58.
Fisher, A.J., and Franklin, K.A. (2011). Chromatin remodelling in plant light signalling. Physiologia plantarum 142, 305-313.
Foyer, C.H., Neukermans, J., Queval, G., Noctor, G., and Harbinson, J. (2012). Photosynthetic control of electron transport and the regulation of gene expression. Journal of experimental botany 63, 1637-1661.
Franklin, K.A., and Quail, P.H. (2010). Phytochrome functions in Arabidopsis development. Journal of experimental botany 61, 11-24.
Galvao, V.C., and Fankhauser, C. (2015). Sensing the light environment in plants: photoreceptors and early signaling steps. Current opinion in neurobiology 34C, 46-53.
Gan, X., Stegle, O., Behr, J., Steffen, J.G., Drewe, P., Hildebrand, K.L., Lyngsoe, R., Schultheiss, S.J., Osborne, E.J., Sreedharan, V.T., Kahles, A., Bohnert, R., Jean, G., Derwent, P., Kersey, P., Belfield, E.J., Harberd, N.P., Kemen, E., Toomajian, C., Kover, P.X., Clark, R.M., Rätsch, G., and Mott, R. (2011). Multiple reference genomes and transcriptomes for Arabidopsis thaliana. Nature 477, 419-423.
Gloggnitzer, J., Akimcheva, S., Srinivasan, A., Kusenda, B., Riehs, N., Stampfl, H., Bautor, J., Dekrout, B., Jonak, C., Jimenez-Gomez, J.M., Parker, J.E., and Riha, K. (2014).

Nonsense-mediated mRNA decay modulates immune receptor levels to regulate plant antibacterial defense. Cell host & microbe 16, 376-390.
Göhring, J., Jacak, J., and Barta, A. (2014). Imaging of endogenous messenger RNA splice variants in living cells reveals nuclear retention of transcripts inaccessible to nonsense-mediated decay in Arabidopsis. Plant Cell 26, 754-764.
Graveley, B.R. (2000). Sorting out the complexity of SR protein functions. RNA 6, 1197-1211.
Harter, K., Talke-Messerer, C., Barz, W., and Schäfer, E. (1993). Light- and sucrose-dependent gene expression in photomixotrophic cell suspension cultures and protoplasts of rape (Brassica napus L.). The Plant Journal 4, 507-516.
Harthill, J.E., Meek, S.E., Morrice, N., Peggie, M.W., Borch, J., Wong, B.H., and Mackintosh, C. (2006). Phosphorylation and 14-3-3 binding of Arabidopsis trehalose-phosphate synthase 5 in response to 2-deoxyglucose. Plant J 47, 211-223.
Heijde, M., and Ulm, R. (2012). UV-B photoreceptor-mediated signalling in plants. Trends in plant science 17, 230-237.
Hoecker, U. (2005). Regulated proteolysis in light signaling. Current opinion in plant biology 8, 469-476.
Hunter, J.D. (2007). Matplotlib: A 2D Graphics Environment. Computing in Science & Engineering 9, 90-95.
Imaizumi, T., Tran, H.G., Swartz, T.E., Briggs, W.R., and Kay, S.A. (2003). FKF1 is essential for photoperiodic-specific light signalling in Arabidopsis. Nature 426, 302-306.
Isken, O., and Maquat, L.E. (2008). The multiple lives of NMD factors: balancing roles in gene and genome regulation. Nature reviews. Genetics 9, 699-712.
James, A.B., Syed, N.H., Bordage, S., Marshall, J., Nimmo, G.A., Jenkins, G.I., Herzyk, P., Brown, J.W., and Nimmo, H.G. (2012). Alternative splicing mediates responses of the Arabidopsis circadian clock to temperature changes. Plant Cell 24, 961-981.
Jean, G., Kahles, A., Sreedharan, V.T., De Bona, F., and Rätsch, G. (2010). RNA-Seq read alignments with PALMapper. Current protocols in bioinformatics / editoral board, Andreas D. Baxevanis ... [et al.] Chapter 11, Unit 11 16.
Jiao, Y., Lau, O.S., and Deng, X.W. (2007). Light-regulated transcriptional networks in higher plants. Nature reviews. Genetics 8, 217-230.
Jiao, Y., Ma, L., Strickland, E., and Deng, X.W. (2005). Conservation and divergence of light-regulated genome expression patterns during seedling development in rice and Arabidopsis. Plant Cell 17, 3239-3256.
Jones, E., Oliphant, T.E., and Peterson, P. (2001). SciPy: Open source scientific tools for Python.
Jung, K.-H., Bartley, L., Cao, P., Canlas, P., and Ronald, P. (2009). Analysis of Alternatively Spliced Rice Transcripts Using Microarray Data. Rice 2, 44-55.
Kahles, A., Ong, C.S., Zhong, Y., and Rätsch, G. (2016). SplAdder: Identification, quantification and testing of alternative splicing events from RNA-Seq data. Bioinformatics 32, 1840-1847.
Kalyna, M., Simpson, C.G., Syed, N.H., Lewandowska, D., Marquez, Y., Kusenda, B., Marshall, J., Fuller, J., Cardle, L., McNicol, J., Dinh, H.Q., Barta, A., and Brown, J.W. (2012). Alternative splicing and nonsense-mediated decay modulate expression of important regulatory genes in Arabidopsis. Nucleic acids research 40, 2454-2469.
Kami, C., Lorrain, S., Hornitschek, P., and Fankhauser, C. (2010). Light-regulated plant growth and development. Current topics in developmental biology 91, 29-66.
Karam, R., Wengrod, J., Gardner, L.B., and Wilkinson, M.F. (2013). Regulation of nonsense-mediated mRNA decay: implications for physiology and disease. Biochimica et biophysica acta 1829, 624-633.
Kikis, E.A., Khanna, R., and Quail, P.H. (2005). ELF4 is a phytochrome-regulated component of a negative-feedback loop involving the central oscillator components CCA1 and LHY. Plant J 44, 300-313.
Lareau, L.F., Inada, M., Green, R.E., Wengrod, J.C., and Brenner, S.E. (2007). Unproductive splicing of SR genes associated with highly conserved and ultraconserved DNA elements. Nature 446, 926-929.

Lau, O.S., and Deng, X.W. (2012). The photomorphogenic repressors COP1 and DET1: 20 years later. Trends in plant science 17, 584-593.
Laubinger, S., Fittinghoff, K., and Hoecker, U. (2004). The SPA quartet: a family of WD-repeat proteins with a central role in suppression of photomorphogenesis in arabidopsis. Plant Cell 16, 2293-2306.
Lepisto, A., and Rintamaki, E. (2012). Coordination of plastid and light signaling pathways upon development of Arabidopsis leaves under various photoperiods. Molecular plant 5, 799-816.
Lin, C., and Shalitin, D. (2003). Cryptochrome structure and signal transduction. Annu Rev Plant Biol 54, 469-496.
Liu, J., Jung, C., Xu, J., Wang, H., Deng, S., Bernad, L., Arenas-Huertero, C., and Chua, N.H. (2012a). Genome-wide analysis uncovers regulation of long intergenic noncoding RNAs in Arabidopsis. Plant Cell 24, 4333-4345.
Liu, M.J., Wu, S.H., and Chen, H.M. (2012b). Widespread translational control contributes to the regulation of Arabidopsis photomorphogenesis. Molecular systems biology 8, 566.
Ma, L., Li, J., Qu, L., Hager, J., Chen, Z., Zhao, H., and Deng, X.W. (2001). Light control of Arabidopsis development entails coordinated regulation of genome expression and cellular pathways. Plant Cell 13, 2589-2607.
Mair, A., Pedrotti, L., Wurzinger, B., Anrather, D., Simeunovic, A., Weiste, C., Valerio, C., Dietrich, K., Kirchler, T., Nagele, T., Vicente Carbajosa, J., Hanson, J., Baena-Gonzalez, E., Chaban, C., Weckwerth, W., Droge-Laser, W., and Teige, M. (2015). SnRK1-triggered switch of bZIP63 dimerization mediates the low-energy response in plants. eLife 4, 489-498.
Mancinelli, A. (1994). The physiology of phytochrome action. In Photomorphogenesis in Plants, Ed 2, K.G. Kendrick RE, ed (Dordrecht, The Netherlands: Kluwer Academic Publishers), pp. 211-269.
Mancini, E., Sanchez, S.E., Romanowski, A., Schlaen, R.G., Sanchez-Lamas, M., Cerdan, P.D., and Yanovsky, M.J. (2016). Acute Effects of Light on Alternative Splicing in Light-Grown Plants. Photochemistry and photobiology 92, 126-133.
Mano, S., Hayashi, M., and Nishimura, M. (1999). Light regulates alternative splicing of hydroxypyruvate reductase in pumpkin. Plant J 17, 309-320.
Mano, S., Yamaguchi, K., Hayashi, M., and Nishimura, M. (1997). Stromal and thylakoid-bound ascorbate peroxidases are produced by alternative splicing in pumpkin. FEBS letters 413, 21-26.
Marquez, Y., Brown, J.W., Simpson, C., Barta, A., and Kalyna, M. (2012). Transcriptome survey reveals increased complexity of the alternative splicing landscape in Arabidopsis. Genome Res 22, 1184-1195.
Marquez, Y., Hopfler, M., Ayatollahi, Z., Barta, A., and Kalyna, M. (2015). Unmasking alternative splicing inside protein-coding exons defines exitrons and their role in proteome plasticity. Genome Res 25, 995-1007.
McKinney, W. (2010). Data Structures for Statistical Computing in Python, 51-56.
Monte, E., Al-Sady, B., Leivar, P., and Quail, P.H. (2007). Out of the dark: how the PIFs are unmasking a dual temporal mechanism of phytochrome signalling. Journal of experimental botany 58, 3125-3133.
Nagatani, A. (2004). Light-regulated nuclear localization of phytochromes. Current opinion in plant biology 7, 708-711.
Nakamura, S., Mano, S., Tanaka, Y., Ohnishi, M., Nakamori, C., Araki, M., Niwa, T., Nishimura, M., Kaminaka, H., Nakagawa, T., Sato, Y., and Ishiguro, S. (2010). Gateway binary vectors with the bialaphos resistance gene, bar, as a selection marker for plant transformation. Bioscience, biotechnology, and biochemistry 74, 1315-1319.
Paik, I., Yang, S., and Choi, G. (2012). Phytochrome regulates translation of mRNA in the cytosol. Proc Natl Acad Sci U S A 109, 1335-1340.
Palusa, S.G., and Reddy, A.S. (2010). Extensive coupling of alternative splicing of pre-mRNAs of serine/arginine (SR) genes with nonsense-mediated decay. The New phytologist 185, 83-89.

Pérez, F., and Granger, B.E. (2007). IPython: A System for Interactive Scientific Computing. Computing in Science & Engineering 9, 21-29.
Petrillo, E., Godoy Herz, M.A., Barta, A., Kalyna, M., and Kornblihtt, A.R. (2014a). Let there be light: Regulation of gene expression in plants. RNA biology 11, 1215-1220.
Petrillo, E., Herz, M.A., Fuchs, A., Reifer, D., Fuller, J., Yanovsky, M.J., Simpson, C., Brown, J.W., Barta, A., Kalyna, M., and Kornblihtt, A.R. (2014b). A chloroplast retrograde signal regulates nuclear alternative splicing. Science 344, 427-430.
Polge, C., and Thomas, M. (2007). SNF1/AMPK/SnRK1 kinases, global regulators at the heart of energy control? Trends in plant science 12, 20-28.
Reddy, A.S., and Shad Ali, G. (2011). Plant serine/arginine-rich proteins: roles in precursor messenger RNA splicing, plant development, and stress responses. Wiley interdisciplinary reviews. RNA 2, 875-889.
Reddy, A.S., Marquez, Y., Kalyna, M., and Barta, A. (2013). Complexity of the alternative splicing landscape in plants. Plant Cell 25, 3657-3683.
Rizzini, L., Favory, J.J., Cloix, C., Faggionato, D., O'Hara, A., Kaiserli, E., Baumeister, R., Schafer, E., Nagy, F., Jenkins, G.I., and Ulm, R. (2011). Perception of UV-B by the Arabidopsis UVR8 protein. Science 332, 103-106.
Ruckle, M.E., and Larkin, R.M. (2009). Plastid signals that affect photomorphogenesis in Arabidopsis thaliana are dependent on GENOMES UNCOUPLED 1 and cryptochrome 1. The New phytologist 182, 367-379.
Ruckle, M.E., Burgoon, L.D., Lawrence, L.A., Sinkler, C.A., and Larkin, R.M. (2012). Plastids are major regulators of light signaling in Arabidopsis. Plant physiology 159, 366-390.
Rühl, C., Stauffer, E., Kahles, A., Wagner, G., Drechsel, G., Rätsch, G., and Wachter, A. (2012). Polypyrimidine tract binding protein homologs from Arabidopsis are key regulators of alternative splicing with implications in fundamental developmental processes. Plant Cell 24, 4360-4375.
Sanchez, S.E., Petrillo, E., Beckwith, E.J., Zhang, X., Rugnone, M.L., Hernando, C.E., Cuevas, J.C., Godoy Herz, M.A., Depetris-Chauvin, A., Simpson, C.G., Brown, J.W., Cerdan, P.D., Borevitz, J.O., Mas, P., Ceriani, M.F., Kornblihtt, A.R., and Yanovsky, M.J. (2010). A methyl transferase links the circadian clock to the regulation of alternative splicing. Nature 468, 112-116.
Schluepmann, H., van Dijken, A., Aghdasi, M., Wobbes, B., Paul, M., and Smeekens, S. (2004). Trehalose mediated growth inhibition of Arabidopsis seedlings is due to trehalose-6-phosphate accumulation. Plant physiology 135, 879-890.
Schluepmann, H., Berke, L., and Sanchez-Perez, G.F. (2012). Metabolism control over growth: a case for trehalose-6-phosphate in plants. Journal of experimental botany 63, 3379-3390.
Schneider, C.A., Rasband, W.S., and Eliceiri, K.W. (2012). NIH Image to ImageJ: 25 years of image analysis. Nature methods 9, 671-675.
Schoning, J.C., Streitner, C., Meyer, I.M., Gao, Y., and Staiger, D. (2008). Reciprocal regulation of glycine-rich RNA-binding proteins via an interlocked feedback loop coupling alternative splicing to nonsense-mediated decay in Arabidopsis. Nucleic acids research 36, 6977-6987.
Sheen, J. (1990). Metabolic repression of transcription in higher plants. Plant Cell 2, 1027-1038.
Sheen, J. (2014). Master Regulators in Plant Glucose Signaling Networks 57, 67-79.
Shen, H., Luong, P., and Huq, E. (2007). The F-box protein MAX2 functions as a positive regulator of photomorphogenesis in Arabidopsis. Plant Physiol 145, 1471-1483.
Shikata, H., Nakashima, M., Matsuoka, K., and Matsushita, T. (2012a). Deletion of the RS domain of RRC1 impairs phytochrome B signaling in Arabidopsis. Plant signaling & behavior 7, 933-936.
Shikata, H., Hanada, K., Ushijima, T., Nakashima, M., Suzuki, Y., and Matsushita, T. (2014). Phytochrome controls alternative splicing to mediate light responses in Arabidopsis. Proc Natl Acad Sci U S A 111, 18781-18786.

Shikata, H., Shibata, M., Ushijima, T., Nakashima, M., Kong, S.-G., Matsuoka, K., Lin, C., and Matsushita, T. (2012b). The RS domain of Arabidopsis splicing factor RRC1 is required for phytochrome B signal transduction. The Plant Journal 70, 727-738.
Sibout, R., Sukumar, P., Hettiarachchi, C., Holm, M., Muday, G.K., and Hardtke, C.S. (2006). Opposite root growth phenotypes of hy5 versus hy5 hyh mutants correlate with increased constitutive auxin signaling. PLoS genetics 2, e202.
Simpson, C.G., Fuller, J., Maronova, M., Kalyna, M., Davidson, D., McNicol, J., Barta, A., and Brown, J.W. (2008). Monitoring changes in alternative precursor messenger RNA splicing in multiple gene transcripts. Plant J 53, 1035-1048.
Somers, D.E., Schultz, T.F., Milnamow, M., and Kay, S.A. (2000). ZEITLUPE encodes a novel clock-associated PAS protein from Arabidopsis. Cell 101, 319-329.
Staiger, D., and Green, R. (2011). RNA-based regulation in the plant circadian clock. Trends in plant science 16, 517-523.
Staiger, D., and Brown, J.W. (2013). Alternative splicing at the intersection of biological timing, development, and stress responses. Plant Cell 25, 3640-3656.
Staiger, D., Zecca, L., Wieczorek Kirk, D.A., Apel, K., and Eckstein, L. (2003). The circadian clock regulated RNA-binding protein AtGRP7 autoregulates its expression by influencing alternative splicing of its own pre-mRNA. Plant J 33, 361-371.
Stauffer, E., Westermann, A., Wagner, G., and Wachter, A. (2010). Polypyrimidine tract-binding protein homologues from Arabidopsis underlie regulatory circuits based on alternative splicing and downstream control. Plant J 64, 243-255.
Sugden, C., Donaghy, P.G., Halford, N.G., and Hardie, D.G. (1999). Two SNF1-related protein kinases from spinach leaf phosphorylate and inactivate 3-hydroxy-3-methylglutaryl-coenzyme A reductase, nitrate reductase, and sucrose phosphate synthase in vitro. Plant physiology 120, 257-274.
Sureshkumar, S., Dent, C., Seleznev, A., Tasset, C., and Balasubramanian, S. (2016). Nonsense-mediated mRNA decay modulates FLM-dependent thermosensory flowering response in Arabidopsis. Nat Plants 2, 16055.
Syed, N.H., Kalyna, M., Marquez, Y., Barta, A., and Brown, J.W. (2012). Alternative splicing in plants--coming of age. Trends in plant science 17, 616-623.
Tanabe, N., Yoshimura, K., Kimura, A., Yabuta, Y., and Shigeoka, S. (2007). Differential expression of alternatively spliced mRNAs of Arabidopsis SR protein homologs, atSR30 and atSR45a, in response to environmental stress. Plant Cell Physiol 48, 1036-1049.
Tepperman, J.M., Zhu, T., Chang, H.S., Wang, X., and Quail, P.H. (2001). Multiple transcription-factor genes are early targets of phytochrome A signaling. Proc Natl Acad Sci U S A 98, 9437-9442.
Thimm, O., Blasing, O., Gibon, Y., Nagel, A., Meyer, S., Kruger, P., Selbig, J., Muller, L.A., Rhee, S.Y., and Stitt, M. (2004). MAPMAN: a user-driven tool to display genomics data sets onto diagrams of metabolic pathways and other biological processes. Plant J 37, 914-939.
Thum, K.E., Shasha, D.E., Lejay, L.V., and Coruzzi, G.M. (2003). Light- and carbon-signaling pathways. Modeling circuits of interactions. Plant physiology 132, 440-452.
van der Walt, S., Colbert, S.C., and Varoquaux, G. (2011). The NumPy Array: A Structure for Efficient Numerical Computation. Computing in Science & Engineering 13, 22-30.
van Zanten, M., Tessadori, F., McLoughlin, F., Smith, R., Millenaar, F.F., van Driel, R., Voesenek, L.A., Peeters, A.J., and Fransz, P. (2010). Photoreceptors CRYTOCHROME2 and phytochrome B control chromatin compaction in Arabidopsis. Plant physiology 154, 1686-1696.
Wachter, A., Rühl, C., and Stauffer, E. (2012). The Role of Polypyrimidine Tract-Binding Proteins and Other hnRNP Proteins in Plant Splicing Regulation. Frontiers in plant science 3, 81.
Wang, X., Wu, F., Xie, Q., Wang, H., Wang, Y., Yue, Y., Gahura, O., Ma, S., Liu, L., Cao, Y., Jiao, Y., Puta, F., McClung, C.R., Xu, X., and Ma, L. (2012). SKIP is a component of the spliceosome linking alternative splicing and the circadian clock in Arabidopsis. Plant Cell 24, 3278-3295.

Wu, H.P., Su, Y.S., Chen, H.C., Chen, Y.R., Wu, C.C., Lin, W.D., and Tu, S.L. (2014). Genome-wide analysis of light-regulated alternative splicing mediated by photoreceptors in Physcomitrella patens. Genome biology 15, R10.

Yakir, E., Hilman, D., Kron, I., Hassidim, M., Melamed-Book, N., and Green, R.M. (2009). Posttranslational regulation of CIRCADIAN CLOCK ASSOCIATED1 in the circadian oscillator of Arabidopsis. Plant physiology 150, 844-857.

Yatsenko, D., Reimer, J., Ecker, A.S., Walker E.Y., Sinz, F.H., Berens, P., Hoenselaar, A., Cotton R.J., Siapas, A.G., and Tolias, A.S. (2015). DataJoint: managing big scientific data using MATLAB or Python. bioRxiv.

Yoine, M., Nishii, T., and Nakamura, K. (2006). Arabidopsis UPF1 RNA helicase for nonsense-mediated mRNA decay is involved in seed size control and is essential for growth. Plant Cell Physiol 47, 572-580.

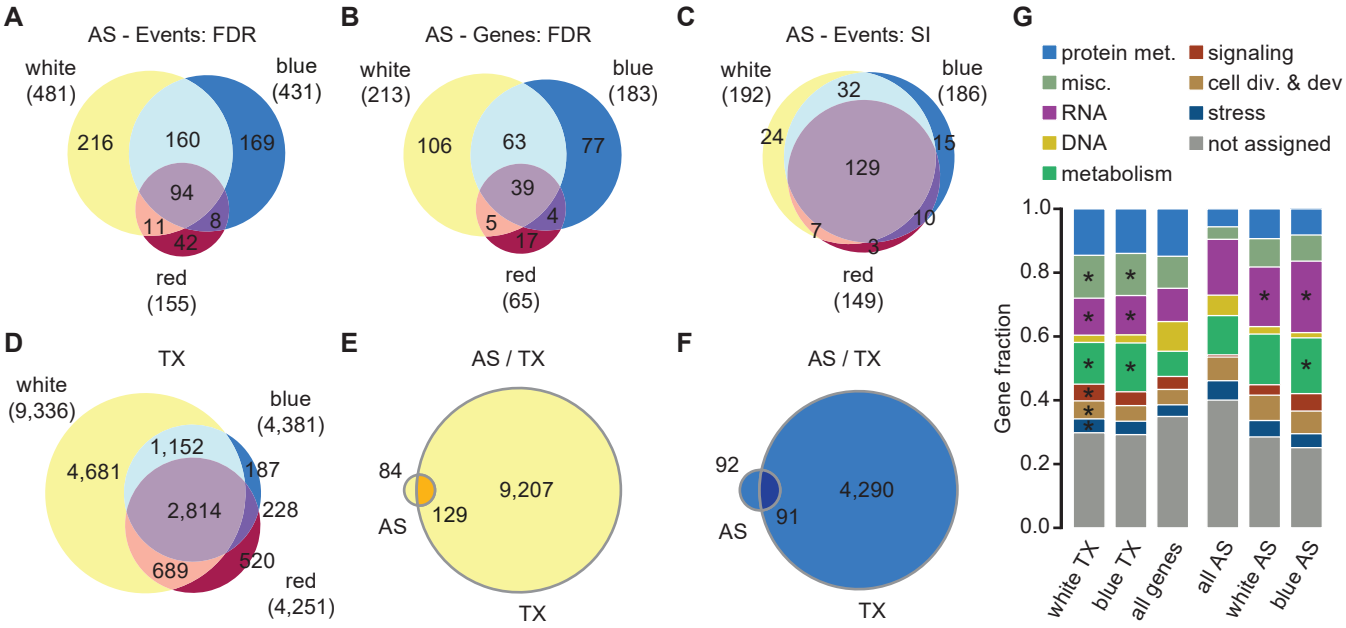

Figure 1. Changes in Alternative Splicing and Gene Expression in the Course of Photomorphogenesis Triggered by Blue, Red, and White Light.

(A, B) Venn diagrams showing the numbers of significantly altered AS events **(A)** and the corresponding numbers of genes affected **(B)** upon 6 h exposure to blue (~6 µmol m^{-2} s^{-1}), red (~14 µmol m^{-2} s^{-1}), and white (~130 µmol m^{-2} s^{-1}) light (FDR < 0.1). Events or genes showing changes in opposing directions under two light conditions were excluded. Total numbers of events/genes changing under each light condition are given in parentheses.

(C) Venn diagram of significantly altered AS events after 6 h light exposure upon additional filtering based on the effect size (change in splicing index, SI > 0.05). Only events with an FDR < 0.1 under at least one light condition were considered for SI analysis. Events with SI changes in opposite directions under two conditions were excluded. Events are grouped according to their SI only.

(D) Venn diagram of genes changing in total expression (TX) upon 6 h exposure to blue, red, and white light (FDR ≤ 0.1). Total numbers of genes changing under each light condition are given.

(E, F) Genes exhibiting changes in AS, TX, or both upon 6 h white **(E)** and blue **(F)** light exposure.

(G) Gene ontology term analysis of genes undergoing AS or TX changes, upon 6 h white or blue light exposure compared to all AS events detected and all genes in MapMan, respectively. met., metabolism; misc., miscellaneous; cell div. & dev., cell division & development; "*" indicate terms overrepresented compared to all AS events and all genes in MapMan, respectively, with Bonferroni-corrected $p < 0.05$.

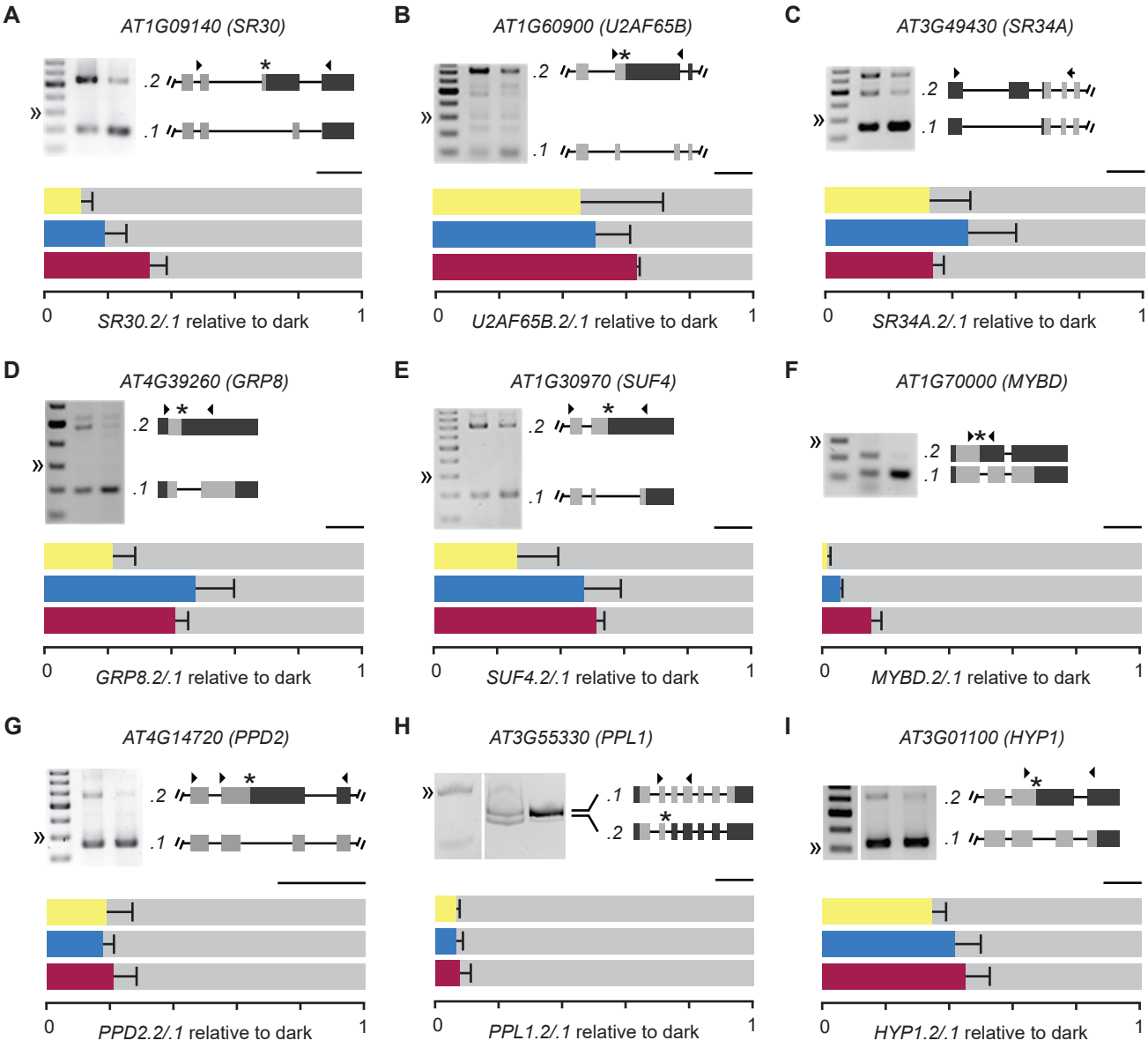

Figure 2. Validation of Light-Dependent Alternative Splicing in Genes from Different Functional Categories.

Splicing variants of genes encoding splicing factors **(A-D)**, putative transcription factors **(E-G)**, a photosynthetic component **(H)**, and a hypothetical chloroplast protein **(I)** were co-amplified from samples grown in darkness and collected at 0 h or after 6 h exposure to white (~130 µmol m^{-2} s^{-1}), blue (~6 µmol m^{-2} s^{-1}), or red (~18 µmol m^{-2} s^{-1}) light (top, middle, bottom bars), and quantified using a Bioanalyzer. Shown are representative agarose gels with double arrowheads pointing at 300 bp of a DNA size ladder with 100-bp increments, and PCR products from 0 h (left) and 6 h white light (right) samples. The variants quantified are labeled (*.1* or *.2*) and partial (A-C, E, G, I) or full (D, F, H) gene models are shown with introns represented by lines and exons by boxes. Regions colored in dark grey are UTRs, and asterisks mark the introduction of a premature termination codon. Solid arrowheads show the positions of the primers used, and the arrow (C) indicates a splice-junction-spanning primer. Bars give average relative splice form ratios with the ratio in darkness set to 1, as indicated by the light grey background bar for each color. Error bars are SD, n = 3. Scale bars beneath the models represent 500 bp.

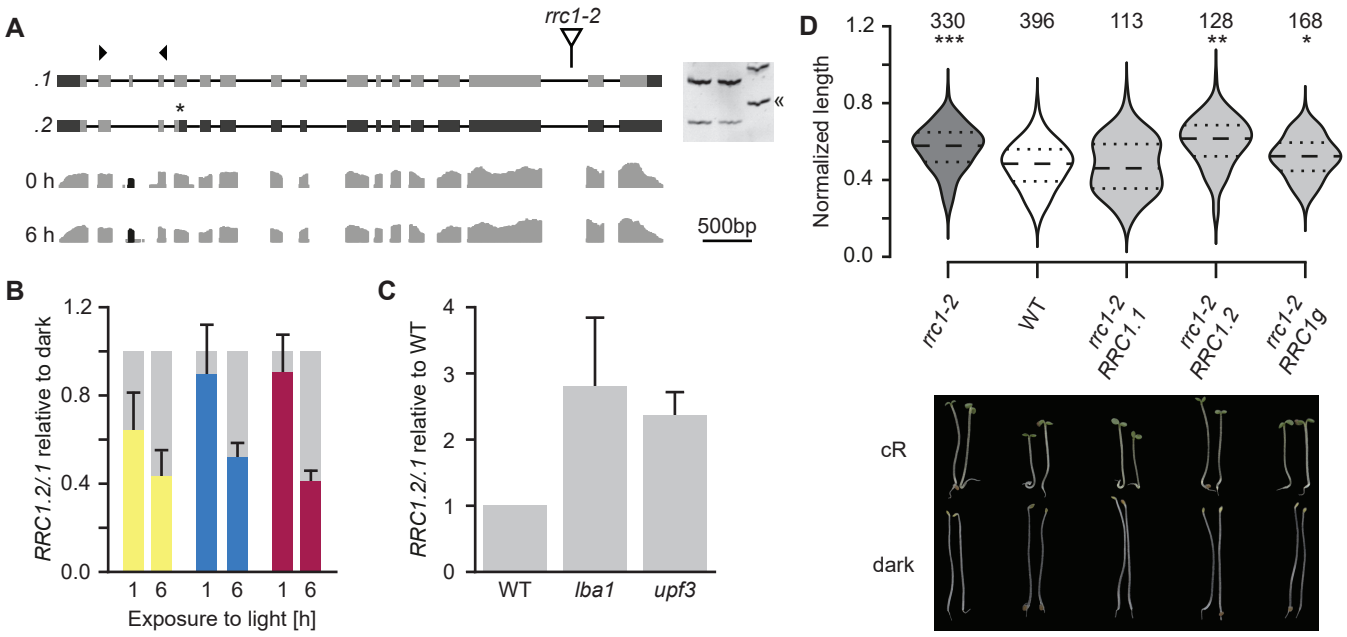

Figure 3. Light Promotes AS of *RRC1* to the Variant Required for Functioning in Phytochrome Signaling.

(A) Models of *RRC1* major splicing variants showing exons as boxes and introns as lines. UTRs are dark grey. The positions of the co-amplification primers are given by arrowheads, and the insertion site of the T-DNA in the *rrc1-2* mutant is indicated. The asterisk marks the introduction of a premature termination codon in the *RRC1.2* variant. The co-amplified PCR products in 0 h (left) and 6 h white light (right) samples separated on a gel are shown with the double arrowhead pointing at 100 bp of a 50-bp ladder. Transcript models are aligned to corresponding amplification products. Below the transcript models, coverage plots show representative RNA-seq results for a 0 h and 6 h light sample. The alternatively spliced region is shown in black.

(B) Confirmation of light-dependent AS under ~130 µmol m^{-2} s^{-1} white (left), ~6 µmol m^{-2} s^{-1} blue (middle), and ~18 µmol m^{-2} s^{-1} red (right) light. Splicing variants were co-amplified from samples grown in darkness for 6 d and collected at 0 h or after 1 h or 6 h exposure to light, and quantified using a Bioanalyzer. Bars give average splice form ratios with the ratio in darkness set to 1. Error bars are SD, n = 3.

(C) Splicing variants were co-amplified from etiolated WT plants, or indicated NMD-deficient mutants, and quantified as in (B). Ratio in WT is set to 1; error bars are SD, n = 3.

(D) Violin plots showing the distribution of the relative hypocotyl lengths measured in red light (~10 µmol m^{-2} s^{-1}) for *rrc1-2*, WT, and complementation lines (top). In each violin the dashed line represents the median, and the dotted lines the quartiles. All hypocotyls were normalized to the average length in darkness of each line. Complementation constructs express tagged splicing variants (*.1*, *.2*) or the genomic sequence (*g*) under control of the CaMV 35S promoter. Asterisks indicate p-values from Mood's median test compared to WT: * < 10^{-2}, ** < 10^{-11}, *** < 10^{-17}. Exact p-values for all comparisons are provided in Supplemental Fig. 6E; n is indicated above each genotype. For each complementation construct, 3 independent F1 lines were each analyzed once in a total of 3 independent experiments. Bottom panel shows representative seedlings from hypocotyl assays in darkness and under red light (cR).

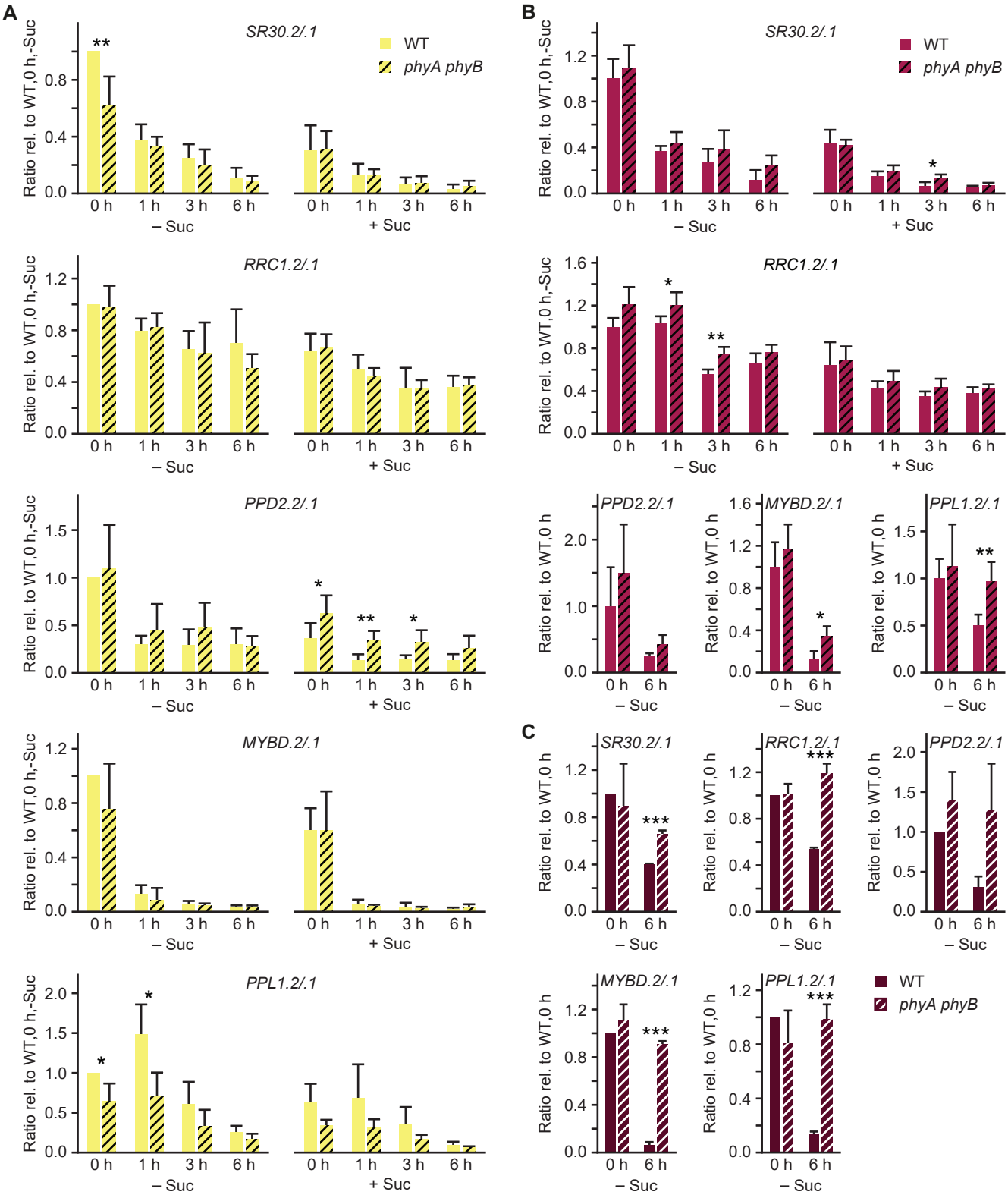

Figure 4. Contribution of Phytochrome A/B Signaling to AS Control Becomes Visible in Red and Far-Red, But Not in White Light.

Etiolated seedlings grown on plates with or without 2% sucrose (Suc) for 6 d were exposed to ~130 µmol m^{-2} s^{-1} white **(A)**, ~28 µmol m^{-2} s^{-1} red **(B)**, or ~15 µmol m^{-2} s^{-1} far-red **(C)** light for the indicated periods. Splice variants were co-amplified and quantified using a Bioanalyzer. AS ratios in (A) and (C) were normalized to the one measured for the corresponding WT 0 h on plates without sucrose, separately for each replicate of WT and *phyA phyB* sample sets. In (B), ratios were normalized to the mean value of the WT replicates at 0 h (- sucrose). Displayed are mean values + SD (A: n = 5-7 for *SR30* and *RRC1*; other candidates: n = 3; B: n = 4 for *SR30*; other candidates n = 3; C: n = 3). p-values: * < 0.05, ** < 0.01, *** < 0.001, comparing WT and *phyA phyB* in an independent t-test, or, if WT is set to 1, in a 1-sample t-test.

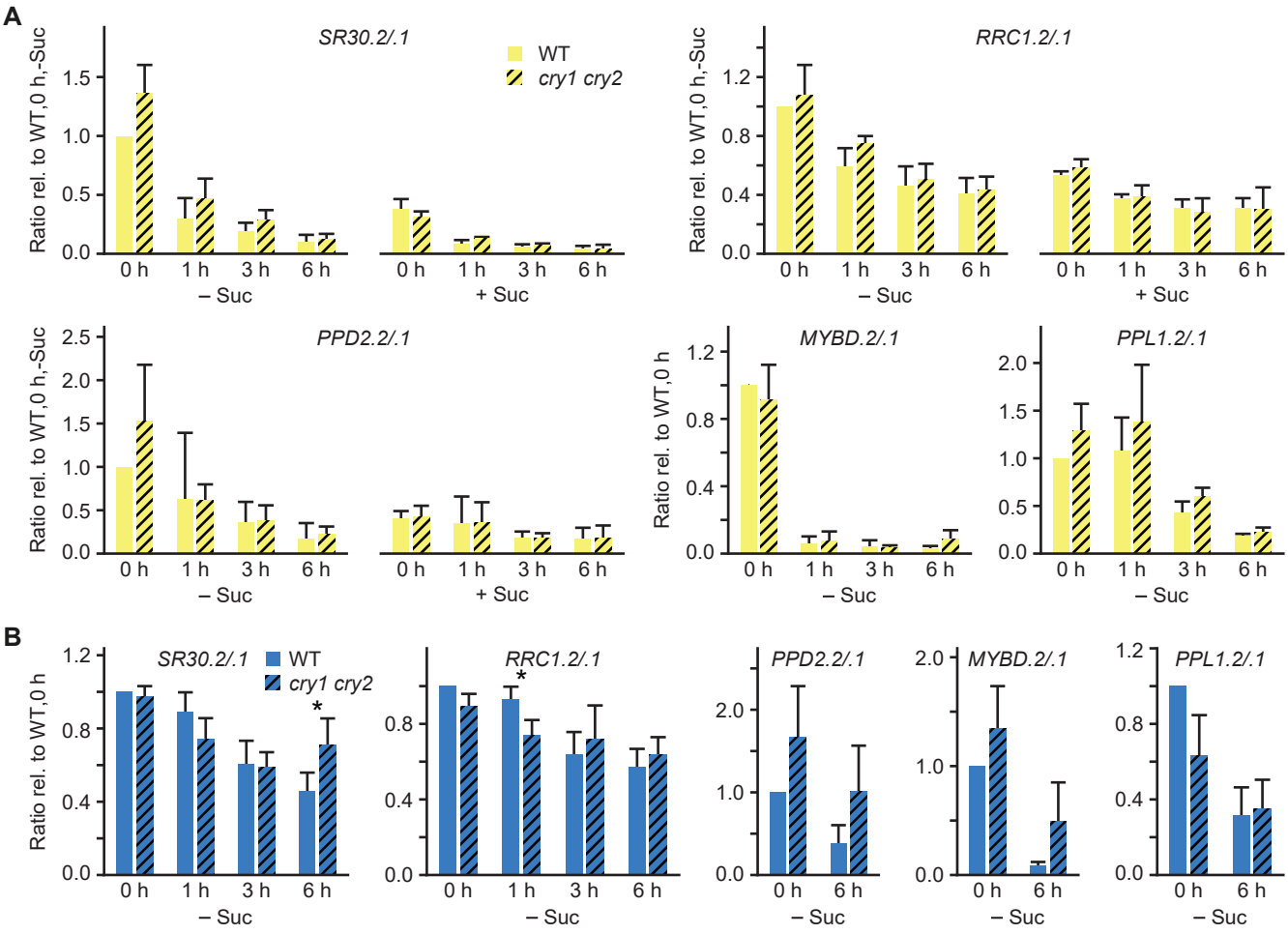

Figure 5. AS Shifts in Response to White Light Are Comparable in WT and *cry1 cry2* Seedlings.

Etiolated seedlings grown on plates with or without 2% sucrose (Suc) for 6 d were exposed to ~130 µmol m^{-2} s^{-1} white **(A)** or ~4 µmol m^{-2} s^{-1} blue **(B)** light for the indicated periods. Splice variants of the indicated genes were co-amplified and quantified using a Bioanalyzer. AS ratios were normalized to the one measured for WT 0 h on plates without sucrose. Displayed are mean values + SD (n = 3-4). Statistical comparison of WT and *cry1 cry2* using independent t-test, or, if WT is set to 1, in a 1-sample t-test (* < 0.05).

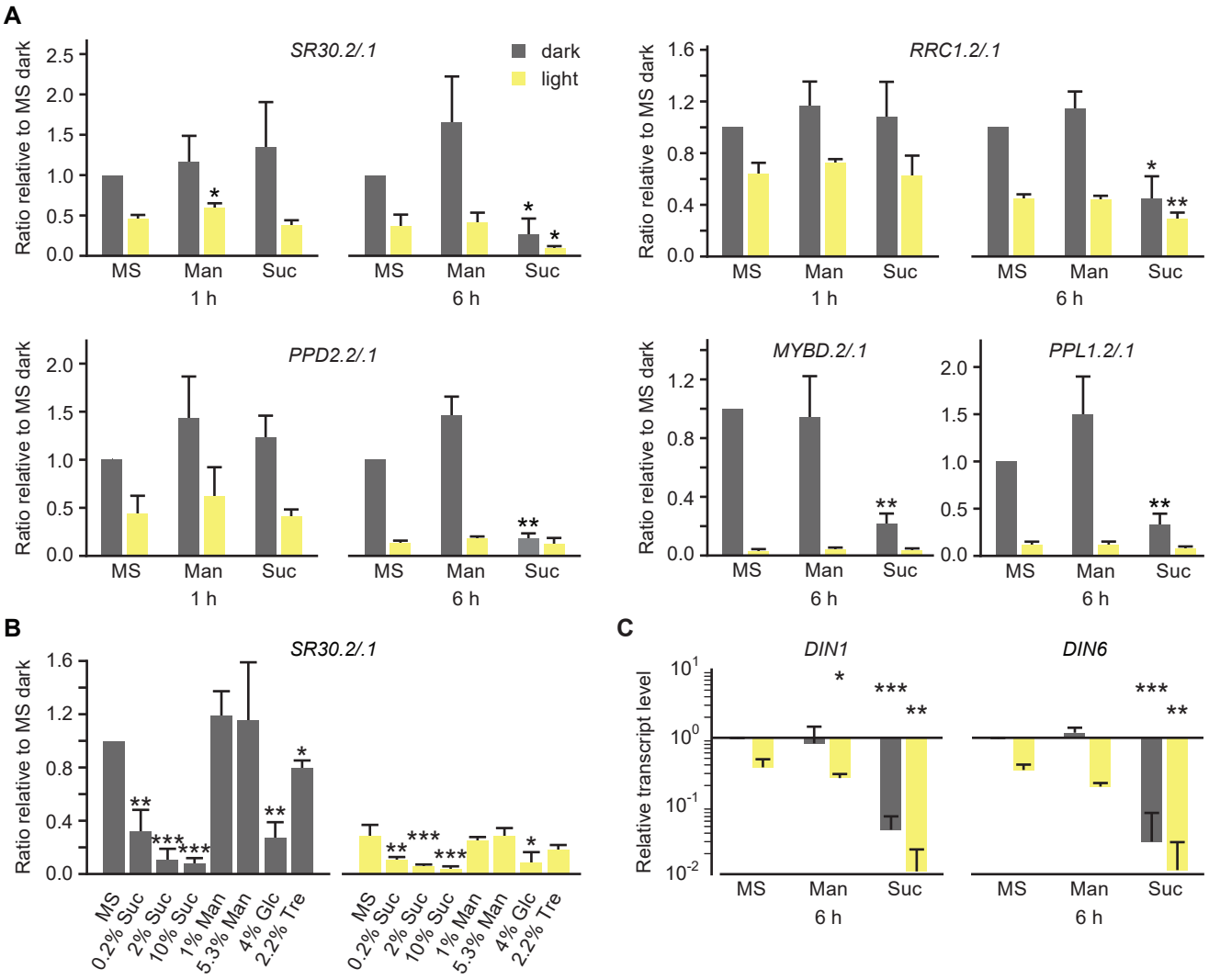

Figure 6. Sucrose and Light Cause Comparable AS Shifts.

(A) Seedlings were grown in darkness for 6 d and afterwards incubated in control medium (MS), mannitol (Man), or sucrose (Suc) solutions for 1 h or 6 h in darkness or ~130 µmol m^{-2} s^{-1} white light. Alternative splice forms were co-amplified and quantified using a Bioanalyzer. Ratios were normalized to the corresponding control samples in darkness. Color scheme for dark (gray) and light (yellow) samples applies to all panels. Displayed are mean values (n = 3). Error bars are SD; p-values: * < 0.05, ** < 0.01, *** < 0.001 comparing Man and Suc to the MS light and dark sample, respectively. Tests are independent t-tests when not tested against 1, and 1-sample t-test when tested against 1. Detailed results from the statistical analysis are provided in Supplemental Table 5.

(B) AS analysis of *SR30* in seedlings grown in darkness and incubated in control medium (MS), sucrose (Suc), mannitol (Man), glucose (Glc), or trehalose (Tre) solutions for 6 h in darkness or ~130 µmol m^{-2} s^{-1} white light. Data are normalized to MS sample in darkness. Displayed are mean values (n = 3-5) + SD. Statistical comparison between MS and different sugars as detailed in (A); dark and light samples were analyzed separately.

(C) RT-qPCR analysis of transcript levels for SnRK1.1 targets. Sample description and data normalization, depiction, and statistical analysis as described in (A). Data displayed on a log scale.

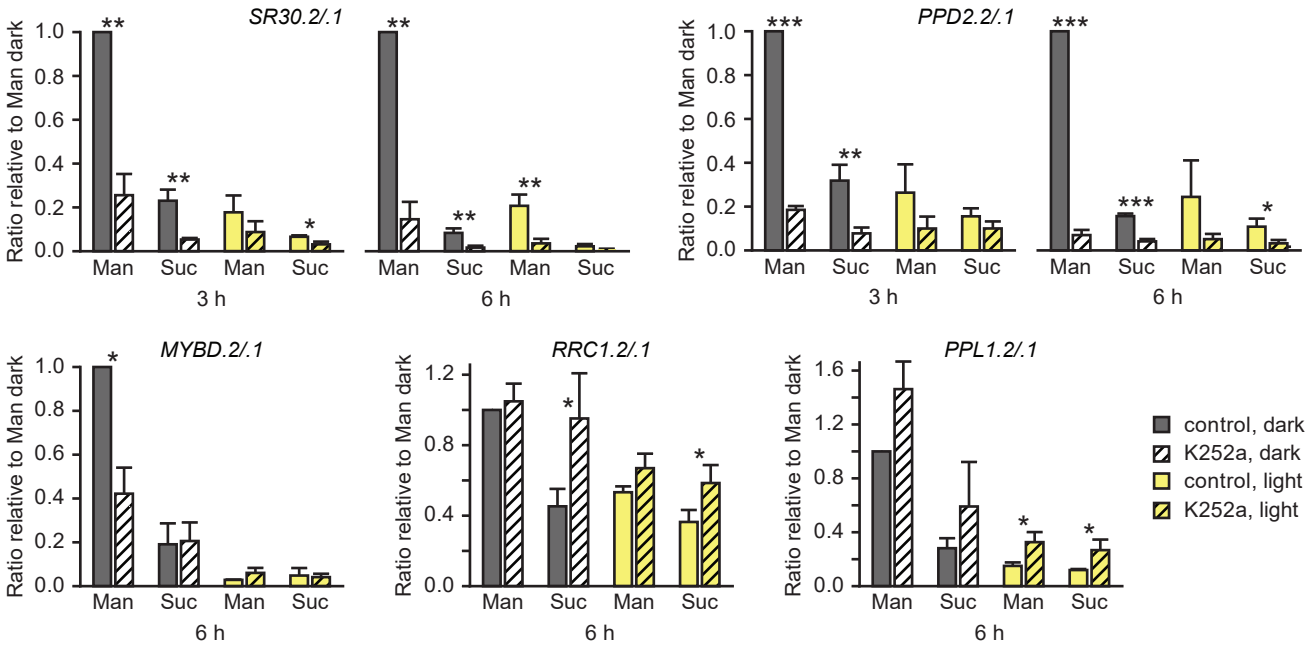

Figure 7. Light- and Sucrose-Regulated AS Involves Kinase Signaling.

WT seedlings were grown in darkness and then incubated in control medium (mannitol, Man) or sucrose (Suc) solution for 3 h or 6 h in darkness or ~130 µmol m^{-2} s^{-1} white light. Incubation was performed in the absence (control) or presence of the kinase inhibitor K252a. AS ratios were determined as described before and are normalized to corresponding Man samples. Displayed are mean values +SD (n = 3); p-values: * < 0.05, ** < 0.01, *** < 0.001 comparing control and K252a treatment. Significant differences determined using independent t-tests when not tested against 1, and 1-sample t-test when tested against 1.

Alternative Splicing Substantially Diversifies the Transcriptome during Early Photomorphogenesis and Correlates with the Energy Availability in Arabidopsis

Lisa Hartmann, Philipp Drewe-Boß, Theresa Wießner, Gabriele Wagner, Sascha Geue, Hsin-Chieh Lee, Dominik M. Obermüller, Andre Kahles, Jonas Behr, Fabian H. Sinz, Gunnar Rätsch and Andreas Wachter

Plant Cell; originally published online November 1, 2016;
DOI 10.1105/tpc.16.00508